

G

of  
les.

# REVIEW OF SCIENTIFIC INSTRUMENTS

**AIP**

a publication of the American Institute of Physics

Model of  
ate samples  
ut the use of  
ment too  
struments.

Review Article: The continuing development of low energy electron microscopy, page 5513

oft,

der in  
ple a host  
image

lateral  
scope  
to  
ssible.

vation.



Vol. 63, No. 12  
December 1992

# The continuing development of low-energy electron microscopy for characterizing surfaces

Lee H. Veneklasen<sup>a)</sup>

*KLA Instrument Company, 3520 Bassett Street, Santa Clara, California 95052*

(Received 15 November 1991; accepted for publication 30 June 1992)

Instrumental aspects of low-energy electron microscopy are reviewed with a view toward the future evolution of this reemergent technology. Both elastically scattered and inelastically excited electrons in the 0–1000-eV range may be used to form direct rather than scanned images of surfaces in the 3–10-nm resolution range. Different instrumental setups may be used to form images that selectively contain information about the topography, crystalline structure, chemical composition, or magnetic orientation of the first few monolayers. Frequently, parallel imaging allows observation of dynamic processes occurring during observation. Key electron optical elements and their systemic relationships are described in the context of a still hypothetical generalized instrument that would allow complementary exploitation of many contrast modes. Image quality issues such as resolution, sensitivity, statistics, and contrast selectivity are considered with a view toward their optimization, in many cases by drawing ideas and technologies from other fields of microscopy.

## 1. INTRODUCTION

The low-energy electron microscope uses the low-energy electrons leaving a surface to form direct rather than scanned images. In the past, this branch of electron microscopy has been called low-energy electron microscopy (LEEM), reflection microscopy, or emission microscopy, depending upon the origin of these electrons. In this article, both the technique and the instrument will be called LEEM because this term does justice to the breadth of the subject, and because instruments using both emitted and reflected electrons share a common evolution and technical foundation.

### A. What is a LEEM?

Figure 1 shows the most important elements of a LEEM alongside a more familiar transmission electron microscope (TEM). Both instruments are the electron optical analog of a light microscope, where a series of lenses project a magnified image upon a screen. Both a LEEM and a TEM use an electron gun to supply electrons that illuminate the sample. Absorption, scattering, and interference of electrons at the sample allow observation of detail much smaller than a light optical microscope can resolve.

A TEM uses high-energy electrons that can pass through a thin sample without losing much energy. Contrast is observed when some electrons are scattered outside the aperture, or when low angle scattered beams interfere with the unscattered beam. The image is a two-dimensional projection of the scattering occurring anywhere within the specimen. In modern TEMs, the specimen lies at ground potential, between the pole pieces of a strong magnetic lens

that is used to focus both the image and illumination.

The LEEM instrument is similar in many ways, but there are important differences that make it suitable for imaging surfaces instead of thin slices of bulk material. Within the objective lens, a strong electric field is applied to the sample surface. Usually the sample is floated at high voltage with respect to the objective lens and the rest of the optics. The low-energy electrons that are either emitted or reflected from the surface are rapidly accelerated, reaching high energy before being refocused by the electron lenses. Low-energy electrons form the image. Light, x rays, heat, and other mechanisms besides electron scattering can generate image electrons. Usually, a LEEM image is formed from electrons that leave the surface with energies between zero and a few hundred eV, and that have been accelerated through a few tens of keV. After acceleration, this image beam still has a spread of energies, but the image can be focused using a narrow range of lens settings. Absorption, emission, scattering, and diffraction properties of the surface may all be used to obtain contrast.

When electrons are used for illumination, the illuminating beam travels coaxially in the opposite direction within the objective lens. It is decelerated before approaching the surface. Low-energy illumination tends to be either reflected or absorbed without penetrating deeply. Similarly, low-energy secondary electrons generated by electron, light, or other illumination cannot escape from deep within the surface, so imaging only involves the immediate surface layer.

The energy of electron illumination is determined by the potential difference between the electron source and sample surface. By adjusting this bias, illumination energy may be varied between zero and a few keV without changing the behavior of the rest of the optics acting upon a much higher energy beam. Using gun bias and an image

<sup>a)</sup> Present address: Etec Systems Inc., 26460 Corporate Ave., Hayward, CA 94545.

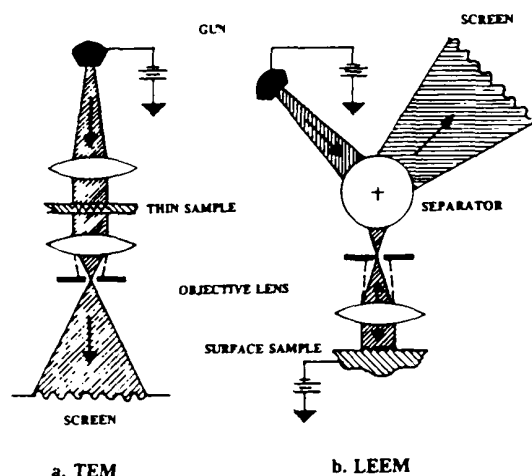


FIG. 1. The basic configurations of TEM and LEEM electron microscopes, emphasizing the two key elements of a LEEM that are necessary for surface imaging.

energy filter, both the illumination and image energies may be selected. Energy relationships are especially important in LEEM, where contrast depends strongly upon the energy of electrons as they enter and leave the surface.

A characteristic feature of the LEEM is the beam separator shown above the objective in Fig. 1(b). This element allows the electron illumination and image beams to fold back upon themselves after reflecting from the surface. The objective lens acts upon incoming illumination and outgoing image beams in very similar ways, but above the objective, a magnetic prism deflects the beams in opposite directions, creating separate spaces for the illumination and imaging optics. In terms of configuration, the main differences between the LEEM and its TEM counterpart are the electrostatic immersion objective lens and the separator, which together allow high-resolution imaging of surfaces using very low-energy electrons.

With this brief introduction to the LEEM, we turn to a more general discussion of surface imaging electron microscopy before returning to a more detailed review of LEEM technology.

## B. Surface imaging microscopy

Surface imaging microscopy helps to visualize or characterize surfaces. A LEEM observes the interface between a solid surface and a vacuum. Usually the first few monolayers of the surface determine its chemical and physical behavior, so this is a region of special interest. At low energy, the mean free path of an electron in a solid varies from 0.5 to 10 nm in the range of 3–1000 eV, with the minimum at about 50 eV.<sup>1</sup> Electron microscopes can thus be very surface selective if low-energy electrons are used for imaging. In this energy range, wavelengths vary from 0.7 to 0.04 nm, i.e., over the range of interatomic and molecular distances. From both direct and diffraction images using this range of wavelengths, one can learn a remarkable amount about a surface.

The information that is desired from an image usually falls into the categories of its topography (shape of the surface) its crystalline structure, its chemical composition, or sometimes its secondary characteristics such as its magnetic domain structure or surface potential. To characterize a surface, one frequently needs to learn something about each of these aspects.

Electrons are a convenient medium to use for high-resolution surface imaging. Their energy and wavelength may be manipulated by electrostatic fields, and they may be focused and deflected by simple electromagnetic elements. Their wavelength has important implications in the way they scatter, and in the available resolution. Even at a low energy of 10 eV, the electron wavelength is about 0.4 nm, suggesting diffraction or uncertainty principle limited resolution on an atomic scale. Due to other electron optical limitations, the realizable LEEM resolution is in the range of 3–10 nm, which still compares favorably with light optical and x-ray alternatives that are fundamentally limited to a few hundred nm.

Direct imaging, rather than electronic reconstruction by scanning, is a characteristic feature of LEEM. Wave optical interference from many sites on the surface may be exploited. Viewing many image elements in parallel, conditions are favorable for the dynamic imaging of changing surfaces. When many pixels are illuminated in parallel, the image contains more electrons from which to gather useful image statistics quickly. The advantages of direct imaging do not preclude the use of scanning microscopy techniques using very similar instrumentation (SLEEM?), but this possibility has yet to be explored. Drawing a parallel from higher energy electron microscopy, one might speculate that both direct and scanning techniques will eventually be applied in LEEM.

A *contrast mechanism* is the way that detail upon the surface is converted to intensity modulation in the image. Given some kind of resolvable difference between regions on the surface, image contrast may be obtained if electrons leave the surface with different intensities, energies, or directions. Heat, photons, molecular beams, ions, or electrons may be used to excite the surface, generating electrons by emission or by reflective scattering. The type and energy of excitation quanta produces different contrast mechanisms. The energy of emitted or scattered electrons may be analyzed to select peaks characteristic of different chemical distributions. The differences in the angular distribution of scattering from individual atoms, or the diffraction due to lattice spacings, are both sources of directional contrast. Lastly, topography, material, local surface potential, and magnetic polarization can all influence the intensity of scattering, which also results in contrast. One recurring theme of this article is the variety and selectivity of different contrast mechanisms available within the instrument.

## C. Surface imaging instruments

Many LEEM contrast mechanisms are also used in other kinds of surface electron microscopes. To help establish the role of LEEM within the broader field of surface

electron microscopy, we compare alternative techniques. Some of the details of the comparison are not within the scope of this review, but the comparison is necessary to establish the role of LEEM within the broader field of surface

The comparison is necessary to establish the role of LEEM within the broader field of surface

The comparison is necessary to establish the role of LEEM within the broader field of surface

The comparison is necessary to establish the role of LEEM within the broader field of surface

The comparison is necessary to establish the role of LEEM within the broader field of surface

The comparison is necessary to establish the role of LEEM within the broader field of surface

The comparison is necessary to establish the role of LEEM within the broader field of surface

The comparison is necessary to establish the role of LEEM within the broader field of surface

electron microscopy, the following paragraphs will compare alternative techniques. First, it is important to list some of the criteria for image quality. Spatial resolution of detail comes to mind first, but alone it is insufficient. Temporal or time resolution measures the rate at which images with useful statistics (signal-to-noise ratio) may be obtained. Where several contrast mechanisms compete, selectivity measures the degree to which contrast may be uniquely interpreted to extract desired information. Lastly, along with spatial and temporal resolution, depth resolution completes the specification of the minimum volume in space/time that can be observed.

The scanning electron microscope (SEM) scans a focused probe of higher energy electrons, typically 1–100-nm diameter at 0.5–50 keV, forming a serial image by collecting reemitted secondary electrons, photons, x rays, characteristic Auger electrons, etc. The resolved volume depends upon the probe diameter and the escape depth of secondary particles. Image statistics usually depend upon the brightness of the electron source, which determines the current that can be concentrated into the small probe.

The scanning tunneling microscope (STM) uses an atomic scale stylus to probe the immediate surface by serving the height of the stylus to maintain constant tunneling current.

Transmission (TEM) and scanning transmission (STEM) microscopes are much higher energy instruments that derive their contrast from low angle scattering occurring unselectively in the bulk or at both surfaces of a thin cross-section sample. Using grazing incidence, they can also exploit specular reflection from surfaces (REM) to see some surface features also visible in LEEM.

All of these instruments play important and sometimes unique roles in surface research, but none can universally characterize surfaces. For example, TEM, STEM, and STM routinely obtain atomic resolution, allowing the localization of individual atoms in molecules and at crystal boundaries. An instrument similar to the STM can even manipulate atoms on cold surfaces. However TEM and STEM are unselective to depth, viewing bulk as a two-dimensional projection. STM is highly surface selective, but has difficulty probing sublayers, and has very limited chemical selectivity. SEM and LEEM do not reach atomic resolution, but in return they offer more opportunities for chemically selective imaging in the 10–100-nm range. Both these instruments use longer wavelength electrons with correspondingly lower diffraction limited resolution. Where inelastic secondary electrons are used, their escape depth also plays a role in limiting lateral resolution.

TEM and LEEM are parallel imaging techniques that view the full field simultaneously. As mentioned previously, it can be shown that under similar coherence conditions, the TEM and LEEM make more quanta available to excite image electrons. They generally offer superior temporal resolution and are attractive for studies involving weak or rapidly changing contrast. Traditionally, SEM and LEEM allow more space for the auxiliary equipment necessary for dynamic studies. However, the serial imaging instruments STEM and SEM tend to be more quantitative

when simpler, single-channel detectors are used. It is not yet clear which instruments are more sensitive to small concentrations of material.

STEM, TEM, SEM, and LEEM can use relatively well understood spectrographic data to interpret chemical contrast. They are all sensitive to characteristic inner shell energy levels, while STM spectroscopy is limited to valence and conduction bands. To some extent, all these instruments suffer from contrast ambiguities due to topography and multiple scattering effects.

TEM and LEEM can use coherent illumination to exploit wave optical interference effects, while the SEM and STM illumination is confined to an individual resolution element. TEM and LEEM can obtain diffraction patterns from localized area, allowing partial reconstruction of the unit cells of crystalline samples, even when they cannot be directly imaged. Holographic imaging techniques are becoming popular in TEM and may also be applicable for some LEEM samples.

LEEM, TEM, STEM, and STM all require rather flat samples for different reasons, making the study of surfaces with macroscopic topography difficult. Special preparation techniques are often required to model real situations. On the other hand, SEM is known for its large depth of field and its tolerance for tilted and even convoluted topography.

From this brief comparison (which may contain generalizations that offend users of each instrument), the point to be emphasized is that each microscope makes unique and complementary contributions to the understanding of surfaces. The LEEM offers a different set of advantages and limitations; its range of possible applications is largely unexplored, so its place among electron microscopes remains for future users to define. The rest of this article will concentrate upon the instrumental aspects of the LEEM, striving to help these future users recognize new opportunities.

#### D. History of LEEM

Evolution of the LEEM spans the history of electron microscopy. Griffith and Engel have recently compiled a fascinating history, recording contributions from fields as diverse as CRT technology and biology.<sup>2</sup> This article will only try to note some of the key advances in the evolution of the modern instrumental configuration. Accompanying progress in applications and other instrumental viewpoints may be found in other reviews.<sup>3–5</sup>

In early thermionic and photoemission microscopes, the advantage of immersing the surface in a high electric field in order to rapidly accelerate electrons was recognized.<sup>6</sup> A two-way coaxial beam of illumination and imaging electrons was applied first for mirror microscopy<sup>7</sup> (where image electrons turn around before reaching the surface), and later, for low-energy electron diffraction.<sup>8,9</sup> A magnetic prism to separate incoming and outgoing beams was first introduced for mirror microscopy,<sup>10</sup> and remains a key feature of all systems using electron illumination. Borrowing from transmission microscopy, as well as from earlier and more specialized mirror microscopes, emission

microscopes, and diffractometers,<sup>10</sup> an objective lens aperture was introduced to enhance resolution and contrast. The first generalized instrument was conceived by Bauer,<sup>11,12</sup> and successfully demonstrated in 1985 by Bauer and W. Telieps.<sup>13</sup> As well as assembling the necessary optical elements, a key advance in this instrument was the use of ultrahigh vacuum technology and the provision for *in situ* preparation and modification of the sample surface. Meanwhile, photoemission applications were extended from metallurgy<sup>4</sup> into biological applications.<sup>14</sup> The advantages of spectroscopic imaging for enhancing both resolution and chemical sensitivity have been recognized,<sup>15,16</sup> but have not yet been realized. These opportunities follow logically from a similar evolution of the SEM and TEM toward analytic capability, and also from well established but nonspatially resolved photoelectron, x-ray (ESCA) and Auger (AEM) spectroscopy. The growing availability of commercial image intensifiers and real time image processors are two examples of advances from outside microscopy that are creating new possibilities in LEEM.

The last few steps in the evolution of the LEEM instrument have not been taken. By analogy with other kinds of electron microscopes, some of these steps are not difficult to predict. Other advances will be determined by specific research tasks for which the instrument seems suitable.<sup>17</sup> Since the evolution of the instrument is driven by a desire to optimally exploit available contrast mechanisms, these will be described before discussing the details of the instrument itself.

## II. RESOLUTION AND CONTRAST IN LEEM

### A. Electron optics of the immersion lens

The basic elements of an electron microscope are an illumination system, magnifying image detection system, and an objective lens containing the sample. Contrast mechanisms may be understood by concentrating upon what happens in the sample and objective lens under specific illumination and imaging conditions. Figure 2 is a schematic representation of the LEEM objective lens, showing electrostatic biasing and the characteristic ray paths of illumination and imaging electrons. The sample is usually floated at a negative potential of 10–30 kV. Facing the surface is a positively biased conical electrode that accelerates electrons away from the surface in an electric field of 10–200 kV/cm. Additional electrodes or magnetic pole pieces, schematically shown as a lens, are used to refocus a magnified image far above the lens. Electrons leave the sample with an initial starting energy  $eV \approx 0$ –1000 eV, but they leave the objective lens with energy  $eV_o \approx 20$  keV, so that although low energies are used at the sample, most of the beam path optics involves fairly high-energy electrons. Since the surface of the sample is the first electrode of the objective, this kind of lens is called an accelerating immersion lens or cathode lens.

Two characteristic ray paths describe the focusing action of the LEEM objective. Imaging rays  $\alpha$  leave the surface from a single point at arbitrary angles. In the absence of lens aberrations, they are all refocused at a conjugate

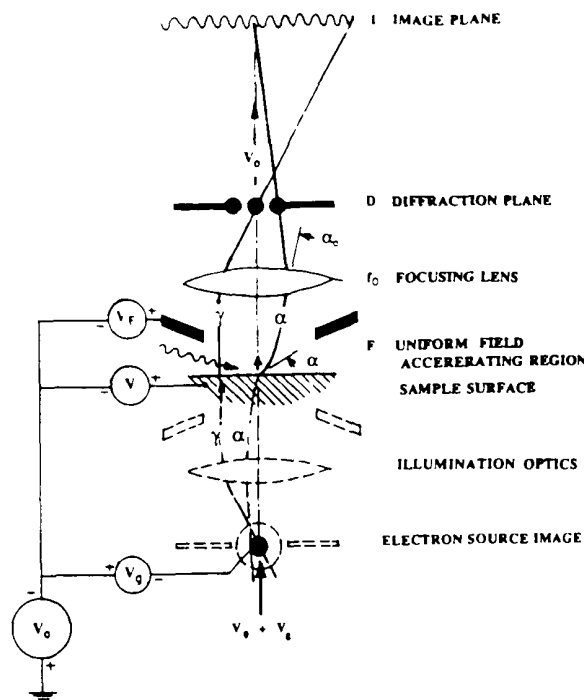


FIG. 2. Schematic diagram of an accelerating immersion lens showing beam energies and the paths of the principle image and field limiting rays in the imaging and illumination optics. In a real system the imaging and illumination rays are coaxial and occupy the space above the sample.

image plane  $I$  above the lens, forming a spatially resolved image. Field rays  $\gamma$  originate anywhere upon the sample, traveling in a specific direction (in this case parallel to the axis). They are refocused at a diffraction plane  $D$  near the exit of the objective lens, forming an angularly resolved image or diffraction pattern. An aperture placed at the diffraction plane limits the angular acceptance and collection efficiency of the lens, while an aperture at the image plane limits its field of view.

In the uniform electric field near the sample surface, slow-moving electrons gain axial momentum while conserving their original radial momentum. They follow parabolic trajectories  $\alpha$  until they enter the nonuniform fields above the first accelerating anode. Here, electrons moving at high energy appear to radiate from a virtual object below the surface. The role of the inhomogeneous field region of the objective lens is to reconverge these rays into a magnified real image. Except for the accelerating region, a LEEM uses the same kind of electrostatic and magnetic lenses found in other electron microscopes.

From Fig. 2, one can see that most of the refraction of LEEM image rays occurs very near the surface. The accelerating region behave like a microlenslet, whose changing index of refraction collimates the beam. When viewed in low voltage space at the surface, the objective appears to have a very short focal length, a large angular aperture, and relatively low aberrations. Thus a strong accelerating field makes possible the remarkably high resolution and collection efficiency of a LEEM operating at very low energy. Since this is often not fully appreciated by electron microscopists familiar with TEM and SEMs that do not

use accelerating lenses, the dependence of resolution and aperture angle upon energy will be discussed in more detail.

During acceleration, the angle  $\alpha$  at initial energy  $V$  decreases to angle  $\alpha_0 \approx \sqrt{V/V_0} \alpha$  at exit energy  $V_0$ . (This is essentially Snell's law in the small angle approximation.) The focal length  $f_0$  of the inhomogeneous field lens focusing the accelerated beam is comparable to the physical size of the lens, i.e.,  $f_0 \sim 0.5$  cm. Viewed at low voltage  $V$ , the apparent focal length of the entire objective scales with the ratio  $\alpha_0/\alpha = \sqrt{V/V_0}$ , so that a typical  $\alpha$  ray focal length for  $V = 10$  eV electrons is about  $100 \mu\text{m}$  if  $V_0 = 20$  keV. The  $\gamma$  rays are not deflected by the parallel field, so the magnification is independent of  $V/V_0$ . A typical objective aperture angle of  $\alpha_0 \approx 2$  mrad corresponds to about  $\alpha = 89$  mrad at low voltage. The collection efficiency for electrons emitted in a cosine distribution of  $\pi$  str is equal to  $\alpha^2$ , and is an important measure of available image intensity. For this example,  $\alpha^2 = 0.79\%$  at  $\alpha_0 = 2$  mrad, and  $20\%$  at  $\alpha_0 = 10$  mrad, which is the typical range in which a LEEM operates.

Both the uniform accelerating field and the nonuniform focusing fields introduce lens aberrations that blur the image when excessively large aperture angles are used. The most important aberration contributions to the diameter  $\delta$  of a resolvable image element on the surface are chromatic aberration  $\delta_c = C_c \alpha \Delta V/V$  and spherical aberration  $\delta_s = C_s \alpha^3$ , where  $\Delta V$  is the energy spread in the image,  $C_s$  and  $C_c$  are aberration coefficients with units of length that scale with  $f_0$ , and where  $C_s$ ,  $C_c$ ,  $\alpha$ , and  $V$  are all referred to sample space. The aberration coefficients scale directly with the size of the region doing the focusing. In LEEM, chromatic aberration is usually dominant because  $\Delta V/V$  is relatively large at low voltage. In addition, there is a fundamental uncertainty principle or diffraction limited contribution  $\delta_d = 0.6 K_\lambda / V^{1/2} \alpha$ , where wavelength  $\lambda = K_\lambda / \sqrt{V}$  depends upon a constant  $K_\lambda = 1.2 \times 10^{-7}$  cm  $\sqrt{\text{eV}}$  that is independent of energy. Since the diffraction contribution decreases with increasing angle, there is an optimum aperture angle,

$$\alpha_{\text{opt}}^2 = 0.6 K_\lambda V^{1/2} / C_c \Delta V, \quad (1)$$

that may be chosen to minimize resolution  $\delta_{\text{opt}}$  in a chromatic limited objective lens.<sup>3,19</sup> This aperture angle may be reinserted into the quadrature sum of resolution contributions to find the best possible resolution for an instrument operating at energy  $V$ :

$$\delta_{\text{opt}} \approx [1.09 K_\lambda^{1/2} C_c^{1/2} \Delta V^{1/2}] V^{-3/4}. \quad (2)$$

For a transmission or scanning electron microscope operating at  $V = V_0 = 20$  keV,  $\Delta V = 0.5$  eV, and  $C_c \approx C_s \approx f_0 = 0.5$  cm. Eq. (2) predicts a resolution of  $1.1$  nm with a collection efficiency of  $\alpha_0^2 = 0.004\%$ .

Suppose that one tries to reduce the energy of this instrument to  $V = 10$  eV without using an accelerating lens, so that the beam passes through the entire objective at  $10$  eV. It would be tempting to scale down the size of the entire lens, but this is not feasible due to field of view and construction tolerance limitations, which also scale.  $C_c$  and

$C_s$  remain approximately equal to the physical scale of the lens, defined here by  $f_0$ . With decreasing energy, the resolution degrades with  $V^{-3/4}$  and the collection efficiency with  $V^{-1/2}$ , resulting in a resolution of only  $335$  nm, at  $0.00009\%$ . Both resolution and image intensity would be unfavorable; a fact that led many microscopists to doubt that very low voltage imaging was practical.

Fortunately for low voltage microscopy, there is a way to scale down aberrations without scaling down the size or field of view of the objective lens. Suppose that one retains the basic operating energy of the instrument at  $V_0 = 20$  keV, but floats the sample at  $-19.990$  kV so that  $V = 10$  eV electrons are imaged. The electrons are accelerated away from the surface in a strong electric field  $F$  (V/cm), reaching energy  $eV_0$  before entering the inhomogeneous field region of the objective lens. Now, the objective may be viewed as two separate lenses acting in series. Bauer has shown that the chromatic and spherical aberration coefficients for a uniform accelerating field are  $C_s = C_c = V/F$  (cm) for electrons leaving at angle  $\alpha$  with energy  $eV$ .<sup>18</sup> To illustrate the scaling effect, assume very approximately that  $F = V_0/f_0 = (40 \text{ kV/cm})$ , so that  $C_s = C_c = f_0(V/V_0)$ . The aberrations of the accelerating region scale down with the voltage ratio  $V/V_0$ , to a magnitude of  $2.5 \mu\text{m}$  in this example!

The aberrations of the inhomogeneous field region of the objective lens also contribute aberrations  $\delta_{so} = C_{so} \alpha_0^3$  and  $\delta_{co} = C_{co} \alpha_0 \Delta V/V_0$ , but they act upon the accelerated beam with angle  $\alpha_0 = (V/V_0)^{1/2} \alpha$ , and energy  $eV_0$ . For purposes of scaling, we will assume that  $C_{so} \approx C_{co} = k f_0$ , where for a well designed unipotential objective lens whose focus is outside its field,  $k$  ranges from about  $1$  to  $10$ . Combining the aberrations of both lens regions, it can be shown that the effective aberration coefficients in low voltage space are  $C_{st} \approx C_{ct} \approx (V/F) [1 + k^2 V/V_0]^{1/2} \approx f_0 V/V_0 [1 + k^2 V/V_0]^{1/2}$ . These aberrations are nearly equal to  $V/F$  when  $V \ll V_0$ . These approximate scaling arguments show that for low initial energies, the resolution of an accelerating immersion lens depends primarily upon the field strength at the surface instead of the details of the focusing region. If the focal length  $f_0$  is seen as a scale factor determining the magnification and field strength, then aberrations scale down with voltage ratio, and high resolution may be reached even at very low energy.

Using Eqs. (1) and (2) and the approximation  $C_{st} \approx C_{ct} \approx V/F$ , that is valid in the limit of low energy, the following expressions estimate the resolution and collection efficiency of a chromatic aberration limited LEEM objective lens:

$$\begin{aligned} \delta_{\text{opt}} &\approx [1.09 K_\lambda^{1/2} \Delta V^{1/2} / F^{1/2}] V^{-1/4}, \\ \alpha_{\text{opt}}^2 &\approx [0.6 K_\lambda F / \Delta V] V^{-1/2}. \end{aligned} \quad (3)$$

Resolution degrades slowly with decreasing energy, and collection efficiency becomes more favorable, to the point where a substantial fraction of low energy emitted or scattered electrons are used to form images.

These are the basic equations for estimating the ultimate resolution of a simple LEEM. It should be pointed

out than when energy filtering is used to suppress chromatic aberration, even higher resolution is possible with little sacrifice of collection efficiency.<sup>19</sup> Similarly, when lower resolution can be tolerated, aperture angle may also be optimized for much higher collection efficiency. Thus Refs. 2 and 19 give somewhat different results. Reference 20 gives optimized examples for some real lenses.

In Eq. (3), the resolution degrades slowly with  $V^{-1/4}$  instead of  $V^{-3/4}$  in the nonaccelerating case. The collection efficiency actually increases with  $V^{-1/2}$ . At the very low energies used in photoemission microscopy, almost all emitted electrons are actually used to form the image. For the 10-eV example above, the resolution and collection efficiency are 7.5 nm and 0.18%, respectively, and low voltage imaging is much more favorable than in the nonaccelerating case. The electric field strength that can be tolerated by the sample surface usually sets the limits for LEEM electron optical performance. The choice of final accelerating energy  $V_0$  is less important. An accelerating immersion objective lens with a high field at the surface is a characteristic feature of a LEEM, and is necessary to exploit all LEEM contrast mechanisms.

Low energy is often necessary for selective imaging of surfaces. The mean free path of a 10-eV electron in a typical solid is less than 2 nm. Visible light illumination yields photoelectrons whose energy cannot exceed about 2 eV. Characteristic x-ray and Auger peaks are usually in the 50–1000-eV range, while diffuse secondary emission peaks in the 5–20-eV range, regardless of illumination energy. Diffraction and interference effects are strongest when the electron wavelength is comparable to atomic dimensions and crystal lattice spacings, usually around 5–10 eV. At low energy, the cross section for the scattering of illumination electrons increases, allowing high contrast and intensity in images. Secondary emission cross sections peak at incident energies below 1000 eV, and elastic backscattering becomes the dominant electron scattering mechanism below about 20 eV.<sup>3</sup> Scattered intensities can exceed 50% in low-energy reflection and are 100% for mirror microscopy. Thus low voltage imaging offers contrast mechanisms that are often inaccessible or much less favorable in high voltage microscopes.

Various photon, x-ray, ion and molecular beams can illuminate the surface from the side of a conical objective lens face. When uncharged, their energies and paths are not influenced by the accelerating field that extracts image electrons. Electron beam illumination enters the objective lens coaxially from above, traveling in the direction opposite that of the image beam. For clarity, Fig. 2 shows the path of illumination electrons in dotted lines below, as though the optics were a mirror image. As well as allowing ray paths to be seen clearly, this figure emphasizes the similarity of the optics to that of a transmission electron microscope with a prefield condensor/objective lens. Illumination electrons originate from a cathode that is usually biased somewhat negative with respect to the sample, so that they can strike the surface at an energy  $eV$ , equal to or greater than the initial image energy  $eV$ . If electrons scatter inelastically, i.e., lose energy before reemerging from the

surface, then they form an image that contains a spectrum of energies ranging from zero up to the illumination energy. Inelastic imaging modes require an energy filter to select an energy band  $\Delta V$  suitable for high-resolution imaging. If electrons scatter elastically, they leave the surface in a narrow energy band whose energy is equal to the illumination energy and whose width is equal to the energy spread of the electron source. Generally, higher illumination energy tends to favor inelastic scattering, while lower energy favors elastic reflection. Below about 20 eV, an energy filter is not required to separate out inelastic scattering,<sup>13</sup> but a filter is necessary to exploit the full range of available contrast mechanisms.

As shown by the  $\alpha_i$  and  $\gamma_i$  characteristic rays in the illumination optics, the angular spread depends upon the size of the electron source image at plane  $D_i$ . The source shown is actually an image of the electron gun crossover projected to plane  $D_i$  by the rest of the illumination optics. By continuing rays  $\gamma_i$  through the surface, one can see that the objective lens forms another image of the source crossover at the image diffraction plane  $D$ . Thus diffraction and elastic reflection imaging, that depend upon angular resolution for contrast, require a small demagnified source image to provide parallel (coherent) illumination at the sample surface. Contrast mechanisms that use inelastically scattered secondary electrons may use a much larger source, because the angle of reemission does not depend strongly upon illumination angle  $\alpha_i$ . This allows more electrons to illuminate each point upon the sample. By controlling the energy and angular spread of electron illumination, different contrast mechanisms may be selected.

The imaging optics are located off the page above the objective shown in Fig. 2. They may be focused to view either the image plane  $I$  or the diffraction plane  $D$ . For direct imaging, an aperture is placed at the diffraction plane or at an equivalent plane further downstream. This limits the angular acceptance  $\alpha$  and the collection efficiency  $\alpha^2$  according to the discussion of resolution above. Up to the limit of resolution, larger apertures allow structure with smaller periodicities to be observed, because the diffraction plane is a section of reciprocal lattice space, i.e., the Fourier transform of the original wave function at the sample surface. If different areas on the sample generate different angular distributions, for example due to diffraction or topography, then an objective aperture produces contrast even if the total scattering is uniform.

## B. Contrast mechanisms

Figure 3 schematically summarizes some of the contrast mechanisms used in LEEM. References 3, 4, and 21 are particularly useful for review of the same basic mechanisms from different viewpoints. These contrast mechanisms are often very specific to the type of sample, as well as the type, energy, and coherence of illumination, the aperturing and image focus, the imaging energy band, and the image processing techniques. In a LEEM, all of these parameters may be made available to the electron microscopist.

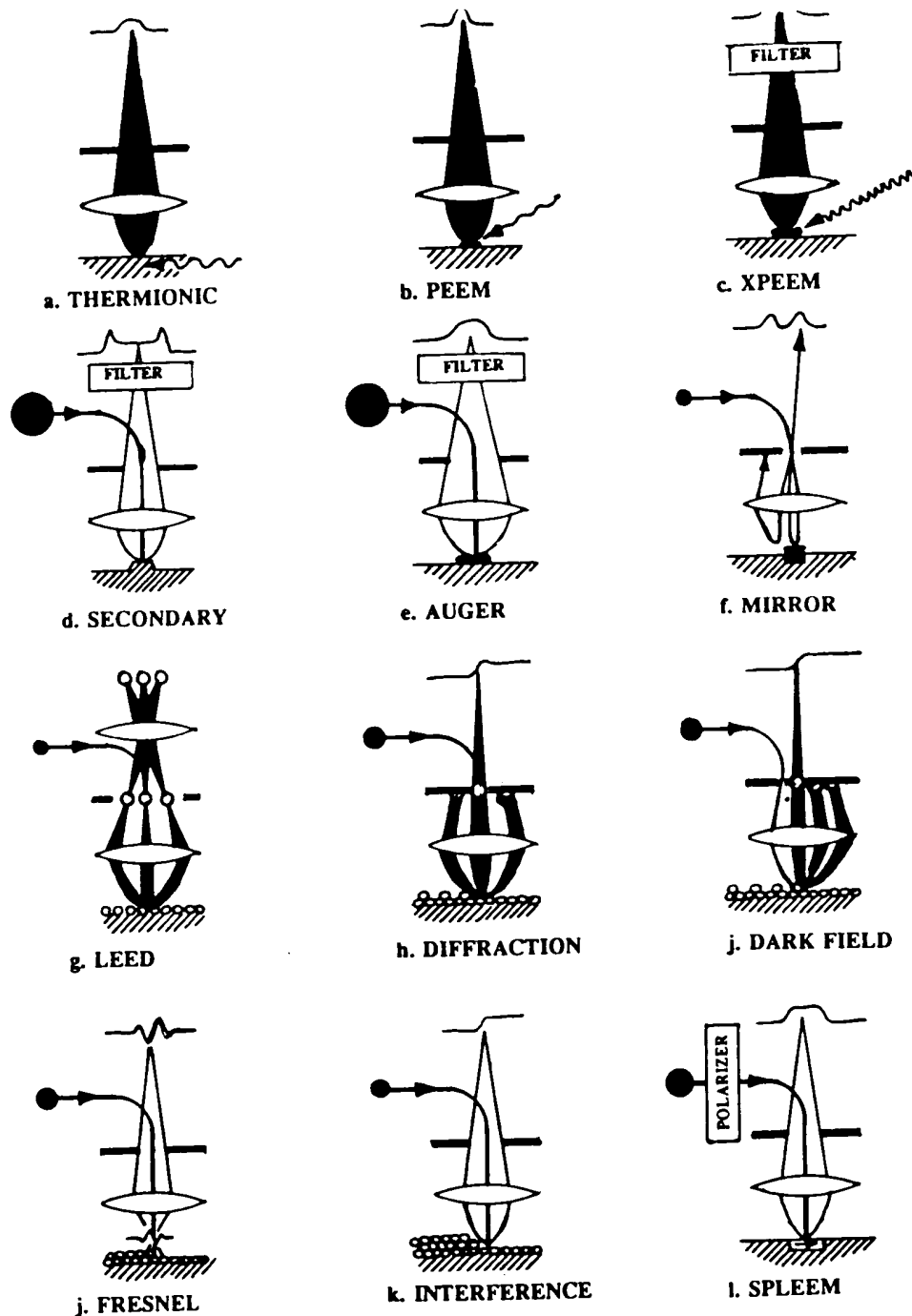


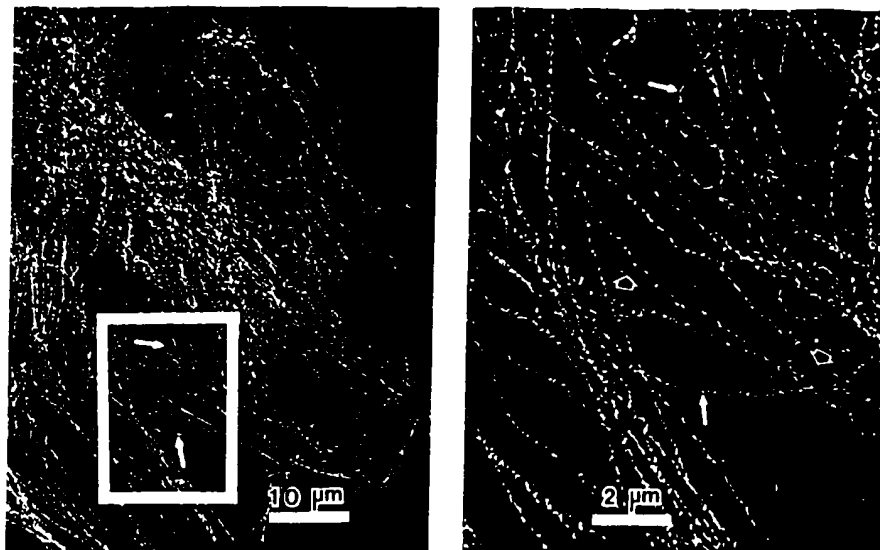
FIG. 3. Some of the contrast mechanisms that are or could be used in LEEM.

The simplest contrast mode is thermionic emission [Fig. 3(a)], where the sample is heated to where electrons can overcome the thermionic work function barrier. The image is a work function map that depends upon the materials, their lattice plane orientations, and their coverage of evaporated or adsorbed material.<sup>4</sup> The range of useful samples is limited by vapor pressures and melting points.

Photoemission microscopy [(PEEM) or PEM, Fig. 3(b)] is obtained using the ultraviolet light illumination from the side. Electron emission is obtained when the photon energy exceeds the threshold for photoelectric emis-

sion, so contrast depends upon both illumination wavelength, material, orientation, and work function.<sup>4,5</sup> Emission thresholds can be very specific to surface chemistry, so this mode typically gives high contrast for suitably matched sources and samples. Sometimes emission is enhanced by coating or chemical labeling using low work function materials.<sup>22</sup> Since both illumination and evaporated coatings come from the side, topography creates shadows that allow three-dimensional visualization. Figure 4 shows a good example of PEEM applied to biological research.<sup>5</sup>





### PEEM - CYTOSKELETAL MICROTUBULES

FIG. 4. Photoemission micrograph illustrating the use of immunogold labeling of microtubules in a cytoskeletal preparation of Swiss 3T3 mouse fibroblast. The low magnification image covers about 1/3 of the cell, showing cytoplasmic space extending outward from the nucleus to the cell boundary. The labeling material selectively bonds to the microtubules, which stand out against unlabeled material. These micrographs demonstrate that topographical and material contrast mechanisms may be used simultaneously to provide information about the distribution of specific subcellular structures. Images of DNA have also been obtained in this instrument. [Courtesy of Griffith (Ref. 71)].

If higher energy soft x-rays are used for illumination, electrons are emitted into a broad energy spectrum that contains both diffuse background and characteristic peaks that depend upon the x-ray ionization cross section for inner shell electrons.<sup>16,23,24</sup> Energies of interest range from about 50 to 1000 eV, and are selected by considering both peak intensity and peak/background ratios. Using an imaging energy analyzer, it should be possible to form an image from characteristic emissions only, by subtracting an image taken at an adjacent energy from one taken at the peak energy. This mode would be called XPEEM or "MicroESCA" [Fig. 3(c)]. Due to the very low quantum yield of characteristic emissions, realization of these images must wait for focused, monochromated x rays derived from intense synchrotron sources.<sup>24,25</sup>

Using a biased electron gun, electron illumination in the 100–2000-eV range produces secondary emission in the 5–20-eV range.<sup>27</sup> This secondary electron contrast [Fig. 3(d)] is equivalent to that used in the SEM. At higher illumination energy, secondary rather than backscatter emissions dominate, and contrast derives from the secondary emission coefficient of the 1–3-nm layer from which secondaries escape. Topographic contrast is enhanced by locally steep inclinations of the surface, where more secondaries escape. The diffuse emission spectrum would require an imaging energy analyzer to suppress chromatic aberration, but given this, spatial and temporal resolution of topography on relatively flat samples could be excellent. The information gained in this mode is expected to be important for sample navigation, instrumental setup, etc.,

where the final goal is to see much less intense images using other inelastic modes.<sup>26</sup> This mode has been demonstrated in a very preliminary way during an evaluation of LEEM for observation of semiconductor wafers and masks.

Higher energy electron beam illumination also excites characteristic Auger electrons that carry information about inner shell energy levels. Both Auger and x-ray emissions are now used in SEM instruments to map elemental distributions. Direct imaging Auger microscopy [Fig. 3(e)] would use characteristic Auger peaks in the 50–1000-eV range, employing the same energy analyzer and image processing techniques described for XPEEM. These two possibilities share the same goal, but are complementary in many respects. X ray and Auger scattering cross sections and signal/background ratios vary widely from element to element. Low contrast will be a challenge to both modes.<sup>19,23</sup> Illumination requirements for Auger imaging should be much simpler and less expensive to meet, and analysis of data can draw from well established scanning Auger microscopy (SAM) methods. Auger and XPEEM contrast modes are two possibilities for "spectroscopic LEEM," which will undoubtedly be the subject of future work.

Spectroscopic LEEM offers some fundamental advantages over scanning alternatives.<sup>19</sup> The useful range of spatial and temporal resolution in a magnified image ultimately depends upon contrast and image statistics, specifically upon the square root of the number of useful electrons per image element that can be collected during a reasonable exposure time. This number is the product of

three factors: illumination dose (number/pixel), useful quantum yield (signal/background contrast  $\times$  quantum yield/str eV), and collection efficiency of the objective lens and energy analyzer optics (str eV). Although the collection efficiency of a LEEM (typically 0.1%–10% depending upon resolution) is lower than scanning detector/analyzers (typically 10%), the LEEM can deliver a much higher dose using an electron gun or x-ray source of limited brightness. This is because many pixels may be illuminated simultaneously. Balancing these two considerations, LEEM may offer faster imaging, especially at high resolution in fields containing many pixels.<sup>26</sup>

For some samples, the proximity effects arising from scattering in adjacent pixels may be smaller using uniform illumination instead of a scanning probe.<sup>26</sup> In SAM, contrast profiles are influenced by the penetration depth of higher energy illumination as well as the escape depth of secondary and Auger electrons. For thin layers of chemical detail on a uniform substrate, this should not be the case in LEEM, because both incident and backscatter electrons passing through the surface are uniformly distributed.

In addition, comparisons of image statistics from different instruments need to be made with specimen damage in mind. Damage depends upon the total dose as well as the rate at which dose is delivered to each pixel. For some samples, damage may be expected to limit the practical resolution and sensitivity of both scanning and direct imaging instruments. In summary, the relative merits of LEEM and SEM for chemical imaging will have to wait for experimental evaluation.

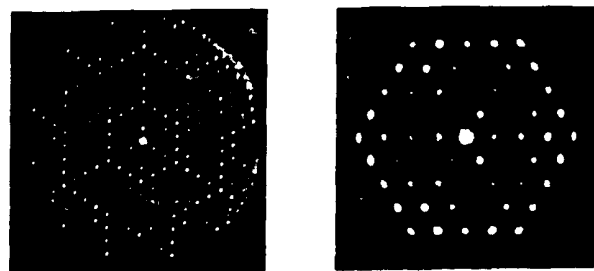
Turning to elastic scattering contrast mechanisms in the LEEM, several unique modes have been used very effectively. Wave optically, each surface atom may be thought of as a generator of spherical Huygen's wavelets that preserve the phase of an incident plane wave. These wavelets recombine to form the object wave function at the surface. Proceeding upwards through the instrument, this wave function is modified by the lens optics. Using the imaging system, the square of the wave function (intensity distribution) may be sampled at any point along its path, including near the surface or at the diffraction plane. With some modifications, the wave optical theory of TEM image formation (e.g., Ref. 28) may be applied to LEEM.

The simplest elastic contrast mechanism is mirror microscopy [Fig. 3(f)], where the electron source is biased slightly positive with respect to the surface. Electrons can either approach very close to the surface before being reflected, or if their energy is very low, they can be absorbed without scattering. Contrast arises if the local potential distribution at the surface is distorted by topography or by local charge. These perturbations can focus, deflect, or capture electrons that would otherwise reflect back up through the aperture. Voltage and topographic contrast may be mixed together unless the surface is (respectively) absolutely conducting or absolutely flat. Excessively large topography can distort the lens action of the accelerating field itself, causing more complicated aberrations.<sup>74</sup> Local field distortions can also deflect electrons leaving the surface with higher energy, causing topographic contrast that

can be confused with chemical or structure contrast. As a broad rule, a LEEM surface should be locally flat to within the expected lateral resolution, although rougher surfaces with lower spatial frequency are tolerable. Surface physics samples usually appear to the eye as a mirror finish. Mirror microscopy has been used to explore topography and also magnetic domains, but it seems to be very difficult to uniquely interpret images. Nevertheless, mirror microscopy might find practical applications in semiconductor inspection and testing.<sup>73</sup>

Low-energy electron diffraction [LEED, Fig. 3(g)] is an established technique that becomes particularly favorable using a LEEM objective lens.<sup>8,9</sup> Diffraction maxima in angular space occur when the periodicity  $x$  of a crystalline surface, and the wavelength  $\lambda = K_\lambda / \sqrt{V}$  of a coherent beam, satisfy the diffraction condition  $\sin \alpha = n\lambda/x$ . The objective lens accelerates the beam while converting the discreet angular distribution to a diffraction pattern at plane  $D$  in Fig. 2. As explained above, the accelerating field collimates the beam according to the ratio  $\sin \alpha_0 / \sin \alpha = \sqrt{V/V_0}$ . Since the wavelength is proportional to  $V^{-1/2}$ , the diffraction condition in accelerated space is  $\alpha_0 = K_\lambda / V_0^{1/2} x$ , and the position of diffraction spots in the diffraction plane is  $K_\lambda f_0 / V_0^{1/2} x$ . The initial energy  $V$  cancels out of the expression, so the location of diffraction maxima on the diffraction plane depends only upon periodicity. The practical advantage is that a very wide range of wavelengths or energies may be used conveniently. The angular resolution of the diffraction pattern is also favorable because of the relative ease with which high coherence illumination and diffraction images may be manipulated in the high voltage optics outside the objective. Periodicities of up to 50 nm have been observed.<sup>29</sup> The intensity of diffraction spots ( $V/I$  curves) depend strongly upon wavelength, and are used to probe details of reciprocal space in both LEED and LEEM instruments. Diffraction can occur only when the wavelength is shorter than the periodicity; a fact that can be used to create strong contrast images. A LEEM is a useful tool for LEED diffraction studies with or without resolvable image detail. Figure 5 shows examples of LEED at two different energies.

Wave optical interference creates several important direct imaging contrast modes. By masking different parts of the diffraction pattern with the aperture, different periodicities are enhanced in the reconstructed image. This diffraction contrast [Fig. 3(h)] is usually formed by masking diffraction spots corresponding to periodicities smaller than the instrument can resolve, so that areas with stronger zero-order diffraction (reflection) appear brighter. The relative intensity of diffracted spots from regions of different crystal structure is maximized by appropriate choice of initial voltage. The aperture may also be centered upon an off-axis diffraction spot while masking the central (0,0) beam, creating dark field contrast [Fig. 3(i)].<sup>30</sup> In either case, when the wavelength is chosen so that only the diffraction from larger periodicities or unit cells is possible, contrast can be very strong. The Clausthal group has used this technique extensively to study the dynamics of surface phase reconstructions.<sup>3,31</sup>



82 eV

4 eV

LEED - Si (111) (7 × 7)

FIG. 5. LEED diffraction patterns from a 6- $\mu$ m region on a {111} silicon crystal with (7 $\times$ 7) surface phase reconstruction. The 82-eV pattern shows the primary reflections due to the lattice periodicity as well as somewhat weaker spots due to the seven lower spatial frequencies in this surface phase. At 4 eV the Ewald sphere contracts, and the primary reflexes can no longer satisfy the Bragg condition, so only the inner part of the pattern is visible. This region is shown magnified on the right, illustrating the angular resolution possible even at low energy. The transition between the two energies requires only a change in sample bias, and a very small change in objective focus to keep the illumination parallel. (Courtesy of M. Mundschau.)

In LEEM, wavelengths are comparable to atomic step heights. Fresnel diffraction effects, generated by interferences between wavelets originating from opposite sides of monoatomic step may be viewed using a slight defocus. This phase or Fresnel diffraction contrast [Fig. 3(j)] has been used to study the dynamics of step motion and surface faceting, which play roles in epitaxial growth and surface catalysis.<sup>32,33</sup> Steps generate interference fringes that extend laterally out to the coherence width of an illuminating wave packet, so when the goal is to resolve closely spaced steps, one may want to adjust coherence to only observe the first maxima and minima of the pattern. It has been shown that the coherence width of the illumination must exceed the resolution of the instrument to make the step visible.<sup>34</sup> Step heights may be estimated by noting the dependence of contrast upon wavelength. Figures 6 and 7(a) show two examples of silicon surface images with both diffraction and phase contrast.

If the surface is viewed as layers of reflecting mirrors made of regular atomic layers, then interference contrast [Fig. 3(k)] can arise between wave fronts reflected from different depths. As shown in Fig. 7(b), interference contrast is sometimes visible in the early stages of epitaxial growth, allowing local variations of coverage to be observed.<sup>3</sup>

Magnetization domains may be selectively observed using spin-polarized electron illumination [SPLEEM Fig. 3(l)]. Contrast arises from variations in backscatter cross section according to the relative alignment of surface magnetization and illumination electron spin vectors.<sup>35</sup> Other kinds of contrast are removed by subtracting two images taken with opposite illumination polarization.<sup>36</sup>

To summarize the discussion of LEEM contrast, the selectivity between available mechanisms is based upon several things. First, the nature and state of the sample surface; its temperature, crystallinity, voltage, magnetism,



DIFFRACTION AND TOPOGRAPHIC CONTRAST  
Si (111) (7 × 7), (1×1)  
V = 10 eV 5  $\mu$ m SQ. FIELD

FIG. 6. An example of LEEM elastic reflection modes applied to the study of crystal surfaces. The two hillocks or pinning center defects are caused by the suppression of sublimation and step migration by CoSi<sub>2</sub> crystals. These are conical terraced formations with closely spaced steps that are not resolved. The topographic contrast is due to deflections in locally nonuniform fields, similar to mirror mode. On the surrounding flat areas, atomic steps form the boundaries for some of the triangular islands of (7 $\times$ 7) surface phase upon the Si(111) (1 $\times$ 1) substrate, illustrating diffraction contrast. [Courtesy of Bauer (Ref. 72)].

and coverage of foreign material. These allow or preclude various contrast mechanisms. Second, the choice of illumination; the kind of particle, its energy or wavelength and coherence, all influence the contrast observed. Third, the imaging system; its focus and energy window are used to select contrast. The ability to vary both illumination and image energy over a wide range is particularly important. Lastly, the image processing algorithm; subtraction, filtering, enhancement, etc., allow different kinds of data to be selected *a posteriori*. Illumination intensity and scattering yield determine the image statistics within each image element. This in turn determines the practical range of both spatial and temporal resolution associated with a given contrast mechanism. The goals of high-speed and high-resolution imaging almost always conflict, but the goal of the instrument design is always to maximize both. There is a wealth of complementary information available from low-energy electrons leaving a surface. This information may be extracted using an accelerating immersion objective lens. Different kinds of information may be selected by varying external bias, illumination, and imaging conditions without changing the geometry of the region occupied by the objective lens and sample. This suggests a very flexible instrument that will be discussed in the next section.

### III. THE LEEM INSTRUMENT

#### A. Configuration and biasing

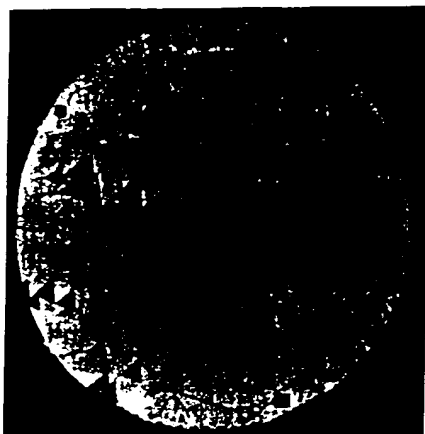
LEEM has evolved as a series of specialized instruments, but it is not necessary to introduce it in the same

FIG. 7. (a) quenching between (7 $\times$ 7) the aperture, monolayers surface and wavelength

way. Inst. that shou above. Tl instrumen tem serve core com ferent app portunitie is emphat ically exi ing eleme existing a 3, 26, 37-

Figur LEEM. T contrast mec stage and magnifyir display sy trast mod lumination

One p the upper vary the strength p + eV of i stant bear lower volt grounds r bias  $V_p$  i which is t tion and sion of Ec



a. DIFFRACTION AND FRESNEL CONTRAST  
Si {111} (7 x 7), (1 x 1)  
V = 10 eV 6  $\mu$ m DIA. FIELD



b. INTERFERENCE CONTRAST  
Mo {110} + Cu  
V = 4 eV 6  $\mu$ m DIA. FIELD

FIG. 7. (a) Shows diffraction contrast between bright areas of Si{111} (7 $\times$ 7) structure and dark areas of a metastable (1 $\times$ 1) phase formed by quenching from 1400 K to room temperature. Fresnel contrast is visible at the step boundary between terraces. The fainter lines are domain boundaries between (7 $\times$ 7) islands, and are believed to be generated by interference between the specular beam and a fractional order reflex that also passes through the aperture. (b) shows interference contrast between step terraces on Mo{110}, whose coverage of evaporated copper varies between 9 and 11 monolayers. Since the crystal structure is identical on all terraces, it is believed that contrast results from interference between reflections from the Cu surface and the Cu-Mo interface. A low energy of 4 eV is chosen to match wavelength with thickness, and to increase penetration, which increases when wavelength exceeds the lattice spacing. (Courtesy of M. Mundschau.)

way. Instead, this article will present the LEEM in a form that should allow all of the contrast mechanisms discussed above. This may or may not be a good way to build an instrument, but the description of such a hypothetical system serves to review the state of development of both its core components and its modular elements specific to different applications. At the same time, future research opportunities and technological needs may become clearer. It is emphasized that only parts of this futuristic system actually exist, but in most cases it seems likely that the missing elements can be built and used effectively. For details of existing and planned systems, the reader is referred to Refs. 3, 26, 37-43.

Figure 8 is a schematic representation of a generalized LEEM. The core subsystems necessary to support all contrast mechanisms include a vacuum chamber, a sample stage and transport system, an objective and additional magnifying lenses, and image detection, processing, and display systems. Specific specimen environments and contrast modes are supported by other modules providing illumination, sample modification, and energy analysis.

One possible high voltage biasing scheme is shown in the upper left. It is desirable to be able to independently vary the initial starting voltage  $V_i$ , the accelerating field strength proportional to  $V_f - V_i$ , and the energy  $eV_i = eV_g + eV$  of illumination electrons, while maintaining a constant beam energy  $eV_0$  in the imaging optics. To do this, lower voltage supplies  $V_g$ ,  $V_i$ , and  $V_f$  are floated with their grounds referred to supply  $V_0 \approx -20$  keV. The first anode bias  $V_f$  is usually chosen to maximize field strength  $F$ , which is the most important parameter influencing resolution and collection efficiency. As explained in the discussion of Eq. (3), the aberrations occurring after acceleration

are usually not as important as those occurring during acceleration, so within limits the choice of  $V_0$  is less critical.<sup>20</sup> Thus it seems desirable to choose a fixed value and then provide for independent adjustment of field strength to accommodate surfaces with different arcover tolerances. Changes in gun voltage and specimen bias are small compared to  $V_0$ , so the biasing scheme shown here allows the energetics at the sample to be adjusted without strongly influencing the focus or alignment of the imaging and energy filter optics.

In the middle of Fig. 8 is the beam separator that creates the Y- or T-shaped beam path characteristic of LEEMs that use coaxial electron beam illumination. Its purpose is to allow the electron illumination and imaging optics to occupy separate spaces, where they can manipulate the two beams without interaction. A magnetic deflection element is required here to deflect incoming and outgoing electrons in opposite directions. A separator is not required for specialized PEEM, XPEEM, or LEED modes.

Upon leaving the separator, the beam enters an intermediate lens system. As well as focusing upon either the magnified image or diffraction plane, this lens system controls magnification and sets up the optical conditions necessary for energy analysis. The complexity of this system depends upon the flexibility and magnification range required. After leaving the intermediate system, the beam enters the energy filter, where electrons outside a narrow energy band are removed from the image. The beam then enters a final projector lens, where the image is further magnified before striking the detector surface.

The intensities of LEEM contrast modes vary widely, so an image intensifier is usually necessary. Ideally, electrons within each resolution element of the image are mul-

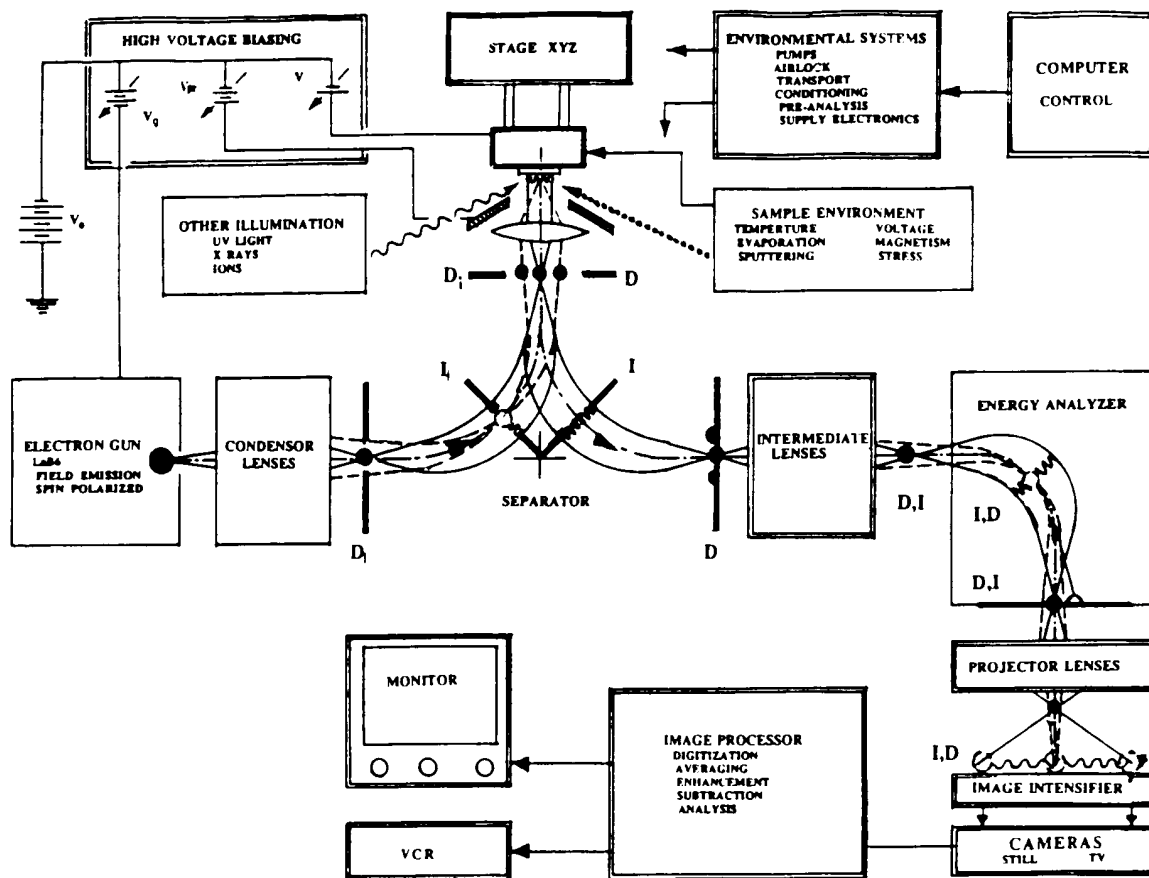


FIG. 8. Schematic diagram of a generalized LEEM showing functional subsystems and options for specific tasks. Modules inside double lines are considered part of the core system or LEEM environment. The positions of important conjugate image and diffraction planes and apertures are shown along the beam path.

multiplied by a uniform and adjustable gain factor, so that the statistics of the intensified image depend only upon quantum noise  $\sqrt{N}$  associated with  $N$  electrons recorded in a detector resolution element during an exposure. The amplified image may be directly photographed or viewed by a TV camera. Digitized video output is stored and processed either in real time or *a posteriori*, after which it may be viewed on a monitor and stored on video tape or disk.

Side mounted illumination and surface modification sources are shown to the left and right of the objective in Fig. 8. They are usually arrayed on a ring of flanges that view the surface at about  $15^\circ$ . Since there are more possibilities than available sites, these sources are usually built in an interchangeable, modular manner. Electron illumination is handled differently, because elastic imaging modes require a parallel, coaxial beam. In Fig. 8 the electron gun and the condenser lens system used to vary its intensity/coherence are shown on the left.

## B. Electron optical configuration

The individual lenses in the optical system may be electrostatic or magnetic. Except for the separator, the optical system bears a strong similarity to analytic transmission electron microscopes, e.g., Ref. 43. The key to understanding the optical system is to identify the location of conju-

gate image and diffraction planes along the beam path. These planes are where focused images of the sample or diffraction plane reappear along the optical path. They are identified by wavy lines for images, and by circles for diffraction planes. Their location and magnification with respect to apertures, the separator, and the energy analyzer are important. The lens elements manipulate the magnification between planes in such a way that when an image plane is magnified, its corresponding diffraction plane is demagnified, and the volume of the beam in position/lateral momentum phase space is conserved.

The location of the conjugate image and diffraction planes shown in Fig. 8 should remain at the same place regardless of image magnification. Within condenser, intermediate, and projector lens groups, there may be other conjugate planes that move around, but for reasons to be explained, the planes shown should remain fixed when focused on the surface. When viewing the diffraction plane, the role of image and diffraction planes following the intermediate lenses are reversed, so that the diffraction pattern is magnified onto the screen. This situation is shown by dotted lines. For scanning LEEM, and for imaging LEEM that requires very intense incoherent illumination, it may also be desirable to form an image of the source on the sample. In this case the roles of image and diffraction

planes  
Th  
LEEM  
aspects  
place t  
separat  
spread  
field d  
large c  
energy  
plane v  
be sho  
tion, a  
here, r  
symme  
inhom  
Sec  
necess:  
shown  
objecti  
interm  
field is  
not be  
Since t  
fixed, s  
image  
try arg  
nificati  
of cert:  
apply t  
and its  
One ca  
tems a  
magnifi  
fraction  
TEM o  
not im  
Th  
a matte  
apertur  
objectiv  
too sm:  
located  
ing it v  
making  
while u  
It can  
inelasti  
source  
separat  
(1 × m  
ations a  
ing the  
area di  
image p  
Las  
to steer  
While  
planes,

planes in the condenser lens optics are also reversed.

The details of the ray optics will be left to TEM and LEEM references,<sup>44</sup> but it is important to mention several aspects that are unique to LEEM. First, it is necessary to place the image from the objective lens at the center of the separator system. This is an achromatic point, where the spread in image energy and small fluctuations in separator field do not degrade the image resolution in spite of its large deflection angle.<sup>45</sup> The same situation applies in the energy analyzer, where any other location of the image plane would cause dispersion in the final image. It can also be shown that this minimizes aberrations such as distortion, astigmatism, and coma.<sup>46</sup> The basic reason is that here, rays that converge to form an image point are anti-symmetric, and close together as they pass through the inhomogeneous fields at the fringe of the separator magnet.

Second, the separator and energy analyzer elements necessarily act as lenses as well as deflectors. The separator shown in Fig. 8 acts as a lens to transfer the image of the objective lens diffraction plane to a plane in front of the intermediate lens optics. The focal length of the separator field is closely coupled with its deflection angle,<sup>47</sup> and cannot be varied without shifting the system's optical axis. Since the location of the objective lens diffraction plane is fixed, so are the locations of the conjugate illumination and image diffraction planes beyond the separator. By symmetry arguments, it has been shown that the optimum magnification of such prism optics is 1:1, allowing cancellation of certain distortion and coma effects.<sup>46</sup> Similar arguments apply to the energy analyzer, which is why the analyzer slit and its conjugate diffraction plane upstream are also fixed. One can see that the condenser and intermediate lens systems are ideally zoom lens combinations that can vary magnification without changing the locations of either diffraction or image planes. This is why modern LEEM and TEM optics<sup>26,39,43</sup> have many lenses whose interactions are not immediately obvious.

The optimum placement of the apertures in a LEEM is a matter for continuing thought. In a TEM, the contrast aperture is located at the diffraction plane just outside the objective lens, because elsewhere its conjugate images are too small. If the contrast aperture in a LEEM is similarly located, it can interfere with incoming illumination, making it very difficult to find and align the beam, and also making it complicated to admit the illuminating beam while using off-axis diffraction spots for dark field imaging. It can also unnecessarily limit illumination intensity for inelastic imaging by artificially limiting the size of the source image shown in Fig. 2. Another option is to use separate gun and contrast apertures at conjugate planes ( $1\times$  magnified) outside the separator.<sup>26</sup> Similar considerations also apply to field limiting apertures used for defining the illumination disk and the area viewed in selected area diffraction. In Fig. 8, these are shown at the fixed image planes within the separator.

Lastly, one might think that it would be very difficult to steer the beam through this noncoaxial optical system. While this can be true, proper placement of conjugate planes, apertures, and alignment deflectors ease the task.

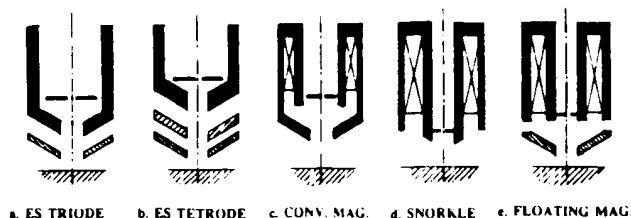


FIG. 9. Some possible objective lens configurations that have been used or proposed for LEEM. Regardless of lens configuration the most important parameter is the field strength at the sample surface. This is controlled by the working distance and the potential difference between the surface and anode facing it. In all cases except a, the field strength may be adjusted according to the tolerance of individual samples, without changing the final beam energy. Cases b and e do not require changes in working distance.

The combination of the separator prism and properly focused objective lens has an important property that can be seen in Figs. 2 or 8. Elastic electrons are reflected in the objective, as though it were an inverting mirror. Electrons entering along a given illumination path emerge along an image path that is an extension of this path, even when the beam is not aimed at the exact center of the objective lens. Since the net transfer through the separator/objective is achromatic, it is much easier to find the beam. Further study of the theoretical and practical characteristics of the overall optical arrangement will make the optical system easier to use. Analogies drawn from TEM experience are useful, and often suggest improvements as well as new imaging modes.<sup>48</sup> One might notice that Fig. 8 could be re-configured as a TEM by replacing the separator by a conventional condenser objective lens. Several combined instruments have been conceptualized.<sup>39,43,48</sup>

### C. Objective lens configurations

Turning to the technology of individual elements, the various objective lens configurations shown in Fig. 9 have been used. Each has an accelerating and focusing region, although they are sometimes superimposed. The *electrostatic triode* [Fig. 9(a)]<sup>18</sup> is the simplest, but it is difficult to obtain maximum field at the surface because even higher field strengths are required inside to have convergent lens action. An *electrostatic tetrode* [Fig. 9(b)]<sup>18,49</sup> allows independent adjustment of field strength and focusing, particularly when the first anode is not grounded.<sup>20</sup> The floating sample may also be placed in front of a *conventional magnetic lens* [Fig. 9(c)],<sup>50</sup> or a single-pole snorkle lens [Fig. 9(d)].<sup>51</sup> In these configurations, the field strength may be varied by moving the sample axially. A magnetic lens with an *electrostatically floating pole piece* [Fig. 9(e)]<sup>20</sup> allows independent adjustment similar to 9(b).

Reference 20 (see also Fig. 10) compares the performance of several LEEM objective lens designs against that of a uniform accelerating field. This uniform field is used as a datum representing the best possible situation, independent of final beam voltage and the details of the lens geometry. The most important conclusion is that at low initial voltages, a high field strength is much more important than either the type of lens or the final voltage. This allows

s are  
shown

ath.  
e or  
are  
dif-  
re-  
alyzer  
nifi-  
image  
ie is  
ion/

tion  
place  
inter-  
ther  
o be  
a fo-  
ane,  
in-  
pat-  
own  
ging  
tion.  
e on  
tion

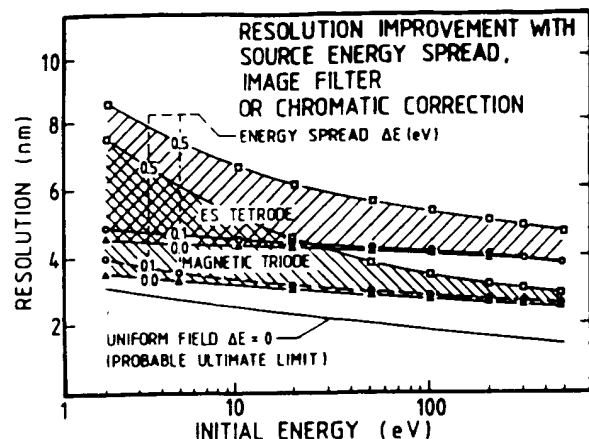


FIG. 10. Computer computations of the ultimate resolution of an electrostatic tetrode and floating pole piece magnetic triode vs initial energy and energy spread at a field strength of 100 kV/cm and final energy of 20 keV. The lowest curve shows the resolution of the uniform electric field portion of the beam path with  $\Delta V=0$ , i.e., when it is only limited by spherical aberration. The details of the lens configuration become more important at higher initial energies, but both lenses would be attractive. The same computations accurately predict the resolution of actual instruments using an electrostatic triode. (From Ref. 20).

considerable flexibility to accommodate other practical concerns. Due to somewhat lower aberrations in the post-acceleration region, magnetic lenses become more attractive at the higher initial energies important for spectroscopic LEEM, but the electrostatic tetrode seems equally attractive for PEEM and low-energy reflection modes. Figure 10 compares the predicted resolution of an electrostatic tetrode [9(b)] and floating pole piece magnetic triode [9(e)] when operating at  $V_0=20$  kV with a realistic field strength of 100 kV/cm. Several values of energy spread  $\Delta V$  are shown as compared with a uniform field at  $\Delta V=0$  that is limited by spherical aberration and diffraction. Energy filtering considerably improves resolution, and within limits, does not degrade collection efficiency because the filter attenuation is compensated by increasing optimum aperture angle [Eq. (3)]. While today's instruments resolve 10–15 nm, 3–5 nm seems to be a realistic goal for the near future.

Correction of both spherical and chromatic aberration would further improve resolution, and even more important, would dramatically increase collection efficiency and reduce dose requirements. In LEEM, several workers have considered the possibility of correctors, applied in conjunction with the separator optics following the objective lens.<sup>39,48,52,53</sup> For example, Rempfer has studied the properties of a hyperbolic mirror placed near an intermediate image of the diffraction plane within the magnetic separator optics. The mirror changes the shape of aberrated wave fronts by introducing negative spherical and chromatic aberration coefficients that can be independently adjusted.<sup>39,52</sup> Conditions in the LEEM seem to favor this kind of correction because relatively low accelerated beam energies are possible, and because sophisticated achromatic, stigmatic prism optics are a necessary part of the optics with or without correction. It would be particularly excit-

ing to try to combine separation, energy analysis, and correction in a single optical concept.<sup>39,48</sup>

#### D. The beam separator

The task of the beam separator is somewhat complex, especially when both elastic and inelastic modes are used. Figure 8 shows that the separator must maintain the alignment of all three beam axes even when illumination and image beam energies differ. The deflection angle of the two legs must be independently adjustable, and their axes of deflection must lie very accurately at the intersection of the three optical axes. In addition, both image and diffraction planes must be faithfully transferred between conjugate planes in the illumination system, through the objective, and then to the intermediate lenses. This is difficult because the focusing action of highly asymmetric magnetic deflectors tends to be very different in the plane of deflection and in the plane perpendicular to it. This can cause both astigmatism and distortion. Since no deflection prism can be free of focusing in both directions, designs strive for equal focusing. What is needed is a separator that behaves like a pair of axially symmetric lenses with curved axes.

Early designs used strong cylindrical lenses (quadrupoles) at the entrance and exit of a single magnetic prism. This can cause large distortions even when the net focusing is free of astigmatism. In a single prism, one cannot obtain the same bending radius for two different beam energies, so the arrangement is also unsuitable for inelastic imaging. One new solution for stigmatic elastic imaging uses a cylindrical electrostatic fringing field to correct asymmetries.<sup>40</sup> Another concept uses three separate prisms with intervening relay lenses.<sup>39</sup> Benefiting from matrix transfer theory,<sup>45,54</sup> and symmetry principles developed by Rose for TEM energy analyzers,<sup>55</sup> the concept of a "close packed prism array" has also been developed and tested.<sup>26,48</sup> In this design, different elements in an array of pole pieces may be excited separately, allowing different energies in the two legs of the beam path. Astigmatism and distortion at all conjugate planes are nearly eliminated by tuning the excitation ratios of inner pole pieces. Reference 48 shows the configuration and first-order properties of several designs.

#### E. Additional lenses

The theory and construction of the condenser, intermediate, and projector lens elements are similar to their TEM counterparts, except that surface physics applications usually require bakable ultrahigh vacuum construction. The goal is zoom lens action while maintaining the position and alignment at conjugate planes along the beam path. The key to reaching this goal is careful attention to mechanical and electromagnetic alignment using appropriate construction techniques, materials, annealing, and magnetic shielding.<sup>38</sup> Computerized control of supply electronics to store and recall focus and alignment setups is almost a necessity.

The concentricity and parallelism of lens elements should be less than about 5  $\mu\text{m}$  in the objective lens, and 20  $\mu\text{m}$  in other lenses. Alignment requirements vary along the

beam aligned that requires gap, to supply age su and so that 1 micros they a essary low-en the qu The c theore succes tics wi use of throug stigma side th posed lenses fields t be fabri stray t multik trarily in the s tion of issue w

#### F. The

Th Its task band w field of viable deflecti in Fig. tions o electro radii of slit con to obta an imag element dispersi smaller

Eiti for ana fraction erration ity crit become exploit symme

sis, and cor-

hat complex,  
des are used.  
in the align-  
mination and  
le of the two  
their axes of  
section of the  
d diffraction  
en conjugate  
he objective,  
icult because  
netic deflec-  
e deflection and  
e both astig-  
mism can be  
ive for equal  
ehaves like a  
axes.

es (quadrupole  
netic prism.  
net focusing  
annot obtain  
energies, so  
atic imaging.  
g uses a cy-  
ect asymme-  
prisms with  
atrix transfer  
by Rose for  
close packed  
ested.<sup>26,48</sup> In  
pole pieces  
nergies in the  
distortion at  
tuning the  
ce 48 shows  
f several de-

enser, inter-  
lar to their  
ics applica-  
m construc-  
ntaining the  
ng the beam  
attention to  
ng appropri-  
ealing, and  
supply elec-  
nt setups is

ns elements  
lens, and 20  
ry along the

beam path, but a good rule is that the beam should be aligned within each lens to about 10% of its diameter, so that the image breathes when its focus is varied. This requires a system of alignment deflectors within each lens gap, to assure alignment of the following lens. Alignment supplies require about  $1:10^4$  stability. Lens and high voltage supply stabilities need to correspond with the analyzer and source energy spread divided by the supply voltage, so that  $1:10^5$ – $2:10^6$  specifications are typical. In transmission microscopy, magnetic electron lenses are favored because they are more compatible with the high-energy beams necessary for resolution. The UHV construction and relatively low-energy beam of a LEEM both justify another look at the question of magnetic versus electrostatic lenses.<sup>26,38,39,42</sup> The choice may be dominated by practical rather than theoretical issues, and both kinds of lenses have been used successfully in LEEMs. Construction of bakeable UHV optics with magnetic lenses is made relatively simple by the use of absolutely nonmagnetic metal liner tubes passing through lens bores. Feedthroughs, connectors, magnetic stigmator/deflectors, and aperture adjustments can be outside the vacuum, and optical elements may be superimposed to minimize path lengths.<sup>26,42</sup> However, magnetic lenses cause image rotation, and can generate stray lateral fields that complicate alignment. Electrostatic lenses may be fabricated very accurately, and are free of rotation and stray fields. This may allow better inherent alignment of multilens zoom modules. They may also be biased arbitrarily with respect to ground potential, allowing flexibility in the sample and optics high voltage design.<sup>38,41</sup> The question of electrostatic versus magnetic lenses is a systemic issue without a simple answer.

#### F. The energy analyzer

The energy analyzer element is necessary for spectroscopic LEEM and desirable for all high-resolution modes. Its task is to filter out electrons outside a narrow energy band without otherwise influencing the aperture angle or field of view. TEM and LEEM literature contains several viable designs using electrostatic, magnetic, or combined deflections.<sup>26,43,45,55,56</sup> The general configuration is shown in Fig. 8, where an analyzer slit blocks off unwanted portions of the beam at a conjugate diffraction plane. Since electrons of differing energy are deflected with different radii of curvature, only those within a band defined by the slit continue into the projector lens. The design problem is to obtain the desired energy resolution while transmitting an image with a sufficiently large number of resolved image elements. This is somewhat easier in a LEEM, because the dispersion (proportional to  $\Delta V/V_0$ ) is larger when  $V_0$  is smaller.

Either magnetic or electrostatic deflection may be used for analysis of full field images. When the image and diffraction planes are properly placed, second-order coma aberrations usually limit the field size. The appropriate quality criteria is the ratio of dispersion to aberration, which becomes more favorable at lower beam energy. One design exploits this by decelerating the beam first, using axially symmetric elements, before applying electrostatic deflec-

tion.<sup>26</sup> Due to the lower accelerating voltages used in LEEM, it is possible that analyzer designs will differ from those used in TEM.<sup>55,56</sup>

One might wonder why the separator in Fig. 8 is not used as an energy analyzer. This is possible for very coarse analysis, but the dispersion of a reasonably sized magnetic separator displaces the image of the diffraction plane by only a few microns per eV of energy spread. The physical diameter  $2\alpha_0 f_0$  of the beam at the objective diffraction plane, and at its 1:1 image after the separator is 20–50  $\mu\text{m}$ , so a slit placed there would artificially limit the aperture angle. In general, it is necessary to demagnify the diffraction plane image in the intermediate system before energy analysis. Principles for optically matching the system for optimum analyzer performance are discussed in Ref. 26.

#### G. Illumination systems

Both thermionic and thermal assisted field emission electron sources have been used in LEEM. The coherence, the total electron current, and the energy spread are all important if the same gun is to be used for elastic and weak inelastic imaging modes. The task of the condenser lens optics is to match the physical size of the emitting area to the desired size of the source image at the diffraction plane of the objective lens. Higher condenser demagnification gives more coherent parallel illumination with less intensity. A small source simplifies the condenser system by avoiding a demagnifying lens, but at least two lenses are needed if a wide range of illumination intensity/coherence is to be available for different contrast modes. A thermionic Lanthanum Hexaboride cathode has proven sufficient for critical diffraction and phase contrast applications,<sup>26</sup> and also offers high current for analytical microscopy and long lifetime in a UHV environment. The field emission sources used in scanning microscopes and high-resolution TEMs do not seem to offer an advantage for the LEEM modes discussed here, but they could prove desirable for future holographic applications.

Illumination conditions at the surface may be directly related to the brightness and energy spread of the cathode, since optical systems conserve these quantities. Electrons leave the surface of a thermionic cathode in a cosine distribution, with an energy spread of about 0.5 eV and a current density of  $J_c = 1$ – $10 \text{ A/cm}^2$ . In the illumination optics, the brightness per eV of energy is conserved, so the current density at the surface may be estimated from the relationship  $J = J_c V_i \alpha_i^2 / \Delta V$ , where  $\alpha_i$  is the angular spread and  $V_i$  is the voltage of the illumination for the contrast mechanism being used. For elastic imaging using LEED, diffraction or Fresnel contrast, illumination angles must be smaller than the angular aperture used for imaging, and current densities of 0.01–0.1  $\text{A/cm}^2$  are typical. For inelastic imaging where illumination angle and energy spread are not constrained, 10–100  $\text{A/cm}^2$  are possible.<sup>19</sup>

Photoemission microscopes use UV lamps with reflective or low loss refractive optics. Deep UV lamps, excimer lasers, and synchrotrons are all used in lithography to generate more intense, higher energy photon illumination. They should become more accessible for LEEM applica-



tions. For spectroscopy, it is desirable for wavelength to be adjustable and monochromatic to optimize signal to background ratio. The useful flux density from these sources depends not only upon their inherent brightness, but also upon the efficiency of lenses, mirrors, and monochromators used to project illumination into the LEEM, so future instruments will undoubtedly favor wide angle elements located as close to the sample as possible.

#### H. Image Intensifiers

The image intensifier is an essential part of the LEEM instrument because intensity varies strongly with the type and coherence of illumination, and the scattering yield for various contrast modes varies over many orders of magnitude. At the final image plane, current in each image element can vary from nanoamperes to a few electrons/s. Frequently small changes in initial energy, aperturing, and illumination produce large excursions, so a wide sensitivity range with automatic adjustment is helpful. Quantitative diffraction and spectroscopy techniques will require a wide and linear dynamic range to accurately record both large contrasts and small differences between image elements. The detector surface and intensifier optics should combine these properties and also resist damage.

There are two basic detector configurations now used in LEEM. In one design, the image falls upon a phosphor screen, whose light output is coupled outside the vacuum through a fiber optics window to an image intensifier and then to a TV camera.<sup>38</sup> Amplification within the sensitivity range of the intensifier/camera combination is electronically adjustable. The other design uses a microchannel plate (MCP) within the vacuum.<sup>57</sup> In an MCP, secondary electrons generated at the cathode surface are amplified inside biased microscopic tubes, and then reaccelerated before striking a phosphor screen that is viewed by a TV camera outside the vacuum.<sup>13</sup>

There is room for improvement in both these arrangements. The key to good image statistics is to utilize every available electron and to amplify it with uniform quantum gain.<sup>58</sup> Phosphor screens degrade the detection quantum efficiency because individual grains have variable light output. MCPs suffer from a low ( $< 1$ ) quantum yield of secondary electrons when used directly in a high voltage beam. The sensitivity range of both arrangements is limited on the high end by saturation and damage effects, and on the low end by thermal noise.

The special requirements of LEEM have generated other suggestions. The DQE of the detector surface can be improved by using YAG or YAP grainless inorganic scintillator disks<sup>59</sup> that are both fast and damage resistant. The sensitivity range may be extended by extracting the light output through a fast, light optical lens that projects a magnified image onto the photocathode of a MCP or other intensifier. These optics allow aperturing to attenuate the image intensity and protect against over exposure. Crossed polarizers with fiber optics coupling might be another alternative. The silicon intensified target used in TV cameras in another alternative, where amplification is obtained by electron hole pair production within a solid-state detector.

In principle, these signals could be captured by a CCD array on the other side of the target. These and other technologies need to be investigated if all contrast modes are to be fully exploited.

#### I. Imaging system

Some of the roles of the digital image processing system have already been discussed. Applications include averaging, contrast enhancement, edge enhancement, real time image subtraction, Fourier analysis, and false color coding. Processed output can also be useful to control automatic focus, stigmation, and alignment routines, and can be used to quantify image resolution and contrast. Suitable systems are in use throughout microscopy. They are becoming faster and cheaper, and will soon be extended to high definition fields.

#### J. Vacuum and specimen manipulation

Surface imaging instruments that are sensitive to submonolayer coverages require ultrahigh vacuum. They generally look more like vacuum chambers than microscopes.<sup>26,38,42</sup> Sample preparation, manipulation, and exchange create engineering challenges. In many cases, it would be desirable to prepare and evaluate samples externally to save instrument time for critical observations. Progress has been made by introducing a multistage airlock and a specimen cartridge that can be preoutgassed and sputtered in an intermediate chamber.<sup>26</sup> In-vacuum transfer from epitaxy and LEED instruments has been suggested, and the advantages of a complementary scanning tunneling microscope observation station have also been recognized.

Specimen motion and vibration control are another challenge made more complicated by the need for UHV and high voltage at the sample. In one instrument,<sup>26</sup> the specimen cartridge is mounted directly upon a multipin high voltage feedthrough with sliding contacts to engage the cartridge. Besides providing electron bombardment heating, thermocouple temperature monitoring, and lens bias connections, this arrangement allows reproducible location of the cartridge with rigid frictional coupling. This insulator is mounted upon a cantilevered bellows which is manipulated in  $X, Y, Z$  and tilt axes by an external stage. The assembly is stabilized by weak frictional coupling to the objective lens, which is vital for eliminating relative vibrational motion. In the mechanical design, it is desirable to use very rigid structures with frictional movements that discourage vibration but allow reasonably fine motions. Stability requirements are comparable to the resolution. Motions smaller than about  $0.5 \mu\text{m}$  may be done by image deflection rather than mechanical control.

For critical surface physics applications, UHV in the low  $10^{-10}$  Torr range is necessary. Ion pumps provide an adequate base vacuum after  $200^\circ\text{C}$  bakeout, but a sublimation pump greatly improves vacuum dynamics. Usually evaporators, sputter guns, and other accessories derive from similar surface physics equipment. Since high temperatures are used during both preparation and observa-

Dion, the cleanliness and purity of cartridge materials are particularly critical. This module should be fully outgassed before introduction into the system.

Used together or in various combinations, the elements discussed above make up a LEEM system. Each element is supported by electronic supplies and a control network.

Ideally the control system is computerized to provide semi-automatic setup and recall of imaging modes, and to allow automated experiments requiring dynamic adjustments or a series of different setups.<sup>26,60</sup>

#### IV. FUTURE DEVELOPMENT AND LIMITATIONS

##### A. At mic imaging and aberration correction

The direct imaging of molecular structure and the motions of atoms and molecules is a continuing challenge in electron microscopy. This has become possible in high voltage TEM and STEM instruments, where images of single molecules in a crystalline array have been reconstructed,<sup>61</sup> arrangements of inorganic atoms near crystal boundaries have been imaged, and the motion of heavy atoms on a substrate have been observed.<sup>62</sup> Major problems include specimen damage and unwanted contrast from underlying substrate material, both of which make the direct imaging of isolated atoms and molecules very difficult.

One might wonder whether this goal might be reached in the low rather than high voltage limit. The traditional (and probably correct) answer is no, because of fundamental resolution limitations, but it seems worthwhile to explore further. In contrast to light optical lenses, whose refractive surfaces can be shaped and positioned to correct geometric and chromatic aberrations, the focusing action of electron lenses is dictated by the equations for electrostatic and magnetic fields in vacuum. They cannot be easily manipulated to correct aberration, so the angle  $\alpha$  in the expression  $\delta_d = 0.6 K_\lambda / V^{1/2} \sin \alpha$  for ultimate diffraction limited resolution must be much smaller to control spherical and chromatic aberration [see Eqs. (1)–(3)]. While a high-resolution light optical lens accepts up to 1 rad, typical electron optical conditions in a TEM operating at 100 keV are  $\alpha = 10$  mrad at  $\delta = 0.2$  nm, and for a LEEM operating at 40 eV,  $\alpha = 56$  mrad, at  $\delta = 4$  nm.<sup>20</sup> Atomic imaging of an atom with diameter of 0.2 nm is not possible at low voltage without aberration correction.

In the absence of aberrations, the situation is different. Assuming for a moment that aberrations can be corrected using mirrors, filters, and/or holographic reconstruction, then both instruments are limited by diffraction. If the optics can accept an angle  $\sin \alpha = 0.6$ , and if there are any electrons scattered at this angle, then the diffraction limit becomes  $\delta_d \approx K_\lambda / \sqrt{V} = \lambda$ , and resolution is only limited by the uncertainty principle. An electron energy of only 36 eV would be required to resolve 0.2-nm atoms. After acceleration to  $V_0 = 100$  keV, the beam angle  $\alpha_0$  is about 10 mrad, and conditions are similar to the high-voltage TEM, so resolution is preserved by the rest of the optics. If the aberrations of the accelerating field could be corrected, atomic resolution could also be possible at low energy.

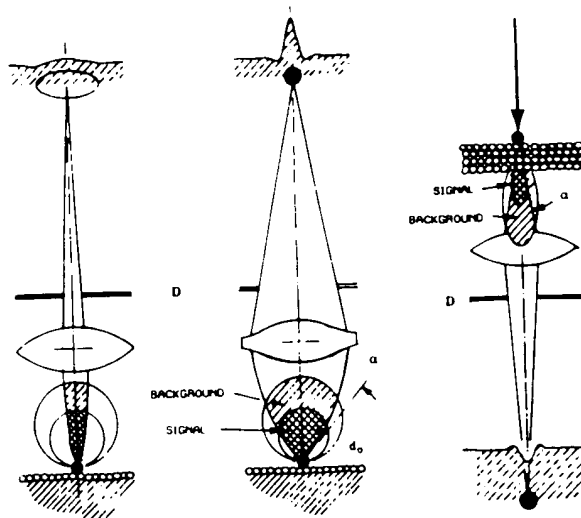


FIG. 11. Scattering angular distributions and imaging ray paths for a discussion of atomic resolution in a hypothetical LEEM with correction of spherical and chromatic aberrations. In the TEM example above 100 keV, scattering angles and useable aperture angles are well matched, allowing atomic resolution without correction. Without correction, the LEEM can neither resolve the atom nor collect a useable signal. With correction this could become possible, and substrate scattering and specimen damage considerations might favor low energy. However, the required corrections are quite extreme, making this scenario unlikely.

Continuing to speculate without practical limitations, one might ask at which energy are contrast, background, and damage conditions more favorable? Consider an isolated atom on an amorphous substrate, illuminated by a parallel beam. The general behavior of the angular scattering distribution is derived in textbooks using both classical and wave optical methods. At low energy where the wavelength is comparable to the atomic diameter, scattering is approximately isotropic. Forward scattering is absorbed in the substrate, and an approximately cosine distribution of backscattered electrons reflects from the surface. A wide angle lens with  $\sin \alpha \approx 0.6$ , placed above the surface, accepts about 50% of the scattered distribution and can resolve the surface atom if the illumination energy exceeds about 36 eV. Figure 11 shows the arrangement, first for an aberration-limited case and then for a purely diffraction limited case necessary for atomic imaging.

At high energy, the scattering angular distribution shifts forward with a mean angle of approximately  $\sin \alpha \approx 0.6 K_\lambda / (\sqrt{V} d_0)$ , i.e., the angle subtended by the Abbe disk of diffraction from a small hole with diameter  $d_0$ . Elastic backscattering decreases sharply, and it is necessary to place the imaging lens below the sample without substantial multiple scattering, the atom of interest must lie on a very thin substrate. A narrow forward peaked distribution emerges. A lens with  $\alpha = \alpha_0$  below the sample also accepts about 50% of the scattering, and can resolve the surface atom. Above about 100 keV this condition can be met with uncorrected objective lenses.

With aberration correction, high and low voltage collection efficiencies are similar, and the intensity of the atom's image depends upon the total scattering cross section. At low energy, this can be a substantial fraction of the atom's physical area  $\pi d_0^2/4$ , as indicated by the fact that backscatters do not escape from below a few monolayers. At high voltage, cross sections decrease, as indicated by the fact that electrons can penetrate many substrate layers without appreciable multiple scattering. Thus one might expect a stronger image signal from the atom of interest when it is illuminated by low voltage electrons.

In both cases, scattering also occurs from substrate atoms, which produces a background that reduces contrast and increases statistical noise. At low voltage, only the first few substrate atoms, lying just below the atom defining an image element, should contribute background. At high voltage, all substrate atoms in the thin sample cross section contribute equally to the background, so unless the substrate is very thin, background scattering should be larger and contrast less favorable.

When specimen damage is important, the ratio of elastic to inelastic damage cross section determines the number of useful image electrons that can be collected before the dose becomes excessive. The author is not aware of data appropriate to very low-energy electrons, but it seems reasonable to expect that low-energy electrons (below the ionization threshold for substantial Auger and x-ray emissions), do less damage. These emissions peak in the 1-keV range, while backscatter cross sections peak at much lower energies.<sup>3</sup>

From these primitive arguments, one concludes that conditions might be favorable for atomic imaging in LEEM were it not for geometric and chromatic aberrations. However, these aberrations are quite fundamental, and in TEM their correction has proved elusive. As energies decrease, the required degree of correction increases. In the 30–100-eV range that might be attractive, aperture angles need to be increased by almost an order of magnitude. This is not seriously contemplated by electron opticians. Nevertheless, there is a relatively large benefit to be gained by correcting aberrations in LEEM, because large angle scattering is there to be exploited. Increases in resolution are accompanied by increases in contrast and image intensity, and corresponding decreases in damage, which is a desirable situation for all contrast modes. This is an important and challenging task for the future.

## B. Additional limiting factors

Specimen damage is a concern in LEEM, especially in photoemission and spectrographic modes with low quantum yields.<sup>4,19,63</sup> Organic samples with weak covalent bonds, or weakly scattering objects that require very high illumination flux are particularly susceptible. Dose per unit area increases with magnification and resolution because the dose per image element remains fixed by statistical requirements, so damage tends to limit useful resolution in biological TEM,<sup>61</sup> and PEEM,<sup>4</sup> and sometimes also in SAM.<sup>63</sup> Choice of illumination energy and maximization of

collection efficiency seem to be the keys to minimizing damage.

Some possible electron optical effects in the LEEM remain to be evaluated. One concern is the interaction between electrons along the beam path. If the density of electrons is high enough to cause statistical deviations in the trajectories of image electrons, both stochastic and chromatic effects degrade resolution.<sup>64</sup> As in electron beam lithography, the microampere beams necessary for spectroscopic LEEM may show these effects. Estimation of beam interactions are difficult in bidirectional beams with wide energy spreads. Recent results suggest that increasing collection angle and reducing angular intensities are particularly effective.<sup>65,66</sup>

Although many contrast mechanisms are understood qualitatively, there is a lack of quantitative theory to help interpret cases where several contrast mechanisms are possible. With quantitative theory, image processing may be applied to the isolation of desired image information. Theory will develop as new observations require interpretation. There are undoubtedly contrast mechanisms that have not yet been recognized. Possibilities for scanning LEEM and holography have been mentioned. Analogy to TEM suggests the possibility of both off-axis full-field holography using beamsplitters,<sup>67</sup> and real time scanning reconstruction using diffraction plane filters.<sup>68</sup> There are also other familiar TEM modes to be tried.<sup>69</sup>

## C. Future development

Although this article presents a rather specific instrumental configuration, there are many possibilities, e.g., Ref. 39. One attractive approach would be to float the electron optical path at positive high voltage, allowing the sample to be grounded.<sup>41</sup> This is advantageous when the sample condition requires special controls, for example, heating, cooling, sputtering, plasma processing, mechanical stress, or application of electrical signals. In principle, the beam path could be confined within an insulating tube along a magnetic beam path, or most of the optics could be electrostatic.<sup>39</sup> As mentioned before, the challenge of combining separation, energy analysis, and correction leaves much room for creativity.

The present state of LEEM's evolution finds a new generation of instruments in a few labs throughout the world.<sup>2</sup> Most of these instruments are laboratory prototypes dedicated to basic research upon specific samples and various combinations of contrast modes. Applications in applied fields such as catalysis, semiconductor process development, quality control, and inspection are just beginning. Since the commercial instrumentation phase is also just beginning, one may speculate about the possible directions it might take.

The core instrument required to exploit each contrast mechanism has a remarkably large fraction of the modules necessary to exploit all of them. This core system is shown in double lined boxes in Fig. 8. If photoemission and elastic electron beam modes are both needed, then the optics and associated electronics approach their full complexity. High-resolution energy analysis is very desirable for all

modes and is necessary for many. Specialization becomes largely a matter of choosing modules that determine sample environment and image processing capability. The major investment seems to be in creating a *LEEM environment*, regardless of the contrast mode. This situation seems to favor generalized instruments in centralized facilities, where they become available to users with a wide variety of research goals.

A designer's challenge is to reduce the complexity of the core system to the point where widespread use in specialized labs becomes realistic. This is a systemic challenge, involving the simplification of each element as well as creative coordination of overall system architecture. It seems likely that a modular approach is desirable, with the core elements being the main target for simplification. Regardless of how this challenge is met, LEEM seems to justify commercial effort toward an instrument suitable for diverse application.

## V. DISCUSSION

One might define a low-energy microscope in two ways. An instrumentalist might prefer: an electron microscope that uses an accelerating immersion cathode lens to form direct images and diffraction patterns from the low-energy electrons leaving a surface. Researchers more concerned with their application might prefer: an electron microscope that can form spatially and temporally correlated images that selectively contain topographic, structural, and chemical information about a dynamically changing surface. The section on contrast mechanisms highlights the variety of information available in LEEM images. In its present state of development, each new sample is an adventure that drives the instrument and techniques a step further. There are many samples waiting to be tried, and doubtless as many surprises waiting, so there is a high level of enthusiasm in the field. The author hopes that this review of the instrumental aspects of LEEM captures some of this enthusiasm.

## ACKNOWLEDGMENTS

The author's experience with LEEM instrumentation derives from a two-year tenure as a visiting scientist at the Technische Universität Clausthal in Germany. Much of the recent development of LEEM in surface science has occurred there, under the direction of Professor Ernst Bauer with his past and present coworkers W. Teliëps, W. Swiech, M. Mundschauf, M. Altman, C. Eisfelder, G. Marx, H. Pinkvos, G. Lilienkamp, and W. Dolinski. The author thanks these people for the opportunity to work with them. R. Phaneuf, E. Williams, and S. Foner are thanked for providing the opportunity to write this article. Scientists at the Institute for Scientific Instruments in Brno, CZ, Fritz Haber Institute in Berlin, University of Oregon in Eugene, and the Institutes for Angewandte Physik in Tübingen and Darmstadt have shared mutual stimulation and encouragement, and will recognize some of their contributions. Much of the historical perspective and compilation of references is due to O. H. Griffith, W.

Engel, and coworkers (Ref. 70), who also organized a recent symposium in Seattle [see *Ultramicroscopy* 36, (1991)]. Although he hopes that they accurately reflect those of the leaders in the field, the author's opinions and ways of viewing the subject are his alone.

- <sup>1</sup>T. Rhodin and J. W. Gadzuk, *Nature of the Surface Chemical Bond* (Eds. Rhodin, Ertl) (North Holland, Amsterdam, 1979), pp. 113-273.
- <sup>2</sup>O. H. Griffith and W. Engel, *Ultramicroscopy* 36, 1 (1991).
- <sup>3</sup>E. Bauer, in *Chemistry and Physics of Solid Surfaces VIII*, edited by R. Vanselow and R. Howe (Springer, Heidelberg, 1991) Springer Series in Surface Sciences, Vol. 22, p. 267.
- <sup>4</sup>R. A. Schwarzer, *Microsc. Acta* 84, 51 (1981).
- <sup>5</sup>O. H. Griffith and G. F. Rempfer, in *Advances in Optical and Electron Microscopy*, edited by R. Barer and V. E. Coslett (Academic, London, 1987), Vol. 10, 269.
- <sup>6</sup>D. B. Langmuir, *Proc. Inst. Radio Eng.* 25, 977 (1937).
- <sup>7</sup>G. Hottenroth, *Ann. Phys.* 30, 689 (1937).
- <sup>8</sup>A. Delong and V. Drahos, *Nature Phys. Sci.* 231, 196 (1971).
- <sup>9</sup>V. Drahos, A. Delong, V. Kolarik, and M. Lenc, *J. Microscopie* (France) 18, 135 (1973).
- <sup>10</sup>V. K. Zworykin *et al.*, *Electron Optics and the Electron Microscope* (Wiley, New York, 1945).
- <sup>11</sup>E. Bauer, *Phys. Rev.* 123, 1206 (1961).
- <sup>12</sup>E. Bauer, in *Proceedings of the 5th International Congress for EM, Philadelphia 1962*, edited by S. Breesee (Academic, New York, 1962), Vol. 1, p. D-11.
- <sup>13</sup>W. Teliëps and E. Bauer, *Ultramicroscopy* 17, 57 (1985).
- <sup>14</sup>O. H. Griffith *et al.*, *Proc. Natl. Acad. Sci. USA* 69, 561 (1972).
- <sup>15</sup>E. Bauer, *Leopoldina Symposium, Physik und Chemie der Kristalloberfläche*, Halle, DDR (1978).
- <sup>16</sup>E. Bauer and W. Teliëps, in *Surface and Interface Characterization by Electron Optical Methods*, edited by A. Howe and U. Valdré (Plenum, New York, 1988), p. 195.
- <sup>17</sup>E. Bauer, M. Mundschauf and W. Swiech, *J. Vac. Sci. Technol. B* 9, 403 (1991).
- <sup>18</sup>E. Bauer, *Ultramicroscopy* 17, 51 (1985).
- <sup>19</sup>L. H. Veneklasen, *Ultramicroscopy* 36, 63 (1991).
- <sup>20</sup>J. Chmelik, L. Veneklasen, and G. Marx, *Optik* 83, 155 (1989).
- <sup>21</sup>M. Mundschauf, *Ultramicroscopy* 36, 29 (1991).
- <sup>22</sup>O. H. Griffith and G. F. Rempfer, *Ultramicroscopy* 24, 299 (1988).
- <sup>23</sup>E. Bauer, *Ultramicroscopy* 36, 52 (1991).
- <sup>24</sup>G. Margaritondo and G. Gerrina, *Nucl. Instrum. Methods A* 291, 26 (1990).
- <sup>25</sup>B. P. Tonner and G. R. Harp, *Rev. Sci. Instrum.* 59, 853 (1988).
- <sup>26</sup>L. H. Veneklasen, *Ultramicroscopy* 36, 76 (1991).
- <sup>27</sup>C. Mollenstedt and F. Lenz, *Advances in Electronics and Electron Physics*, edited by L. Morton (Academic, London, 1963), Vol. 18.
- <sup>28</sup>E. Zeitler and M. G. R. Thompson, *Optik* 31, 258, 359 (1970).
- <sup>29</sup>E. Bauer and R. Phaneuf (private communication).
- <sup>30</sup>W. Teliëps, M. Mundschauf and E. Bauer, *Optik* 77, 93 (1987).
- <sup>31</sup>E. Bauer, M. Mundschauf, W. Swiech, and W. Teliëps, *Ultramicroscopy* 31, 49 (1989).
- <sup>32</sup>M. Mundschauf, E. Bauer, W. Teliëps, and W. Swiech, *Surf. Sci.* 213, 381 (1989).
- <sup>33</sup>R. Phaneuf, N. C. Bartelt, E. Williams, W. Swiech, and E. Bauer, *Phys. Rev. Lett.* 67, 2986 (1991).
- <sup>34</sup>M. Lenc (private communication).
- <sup>35</sup>J. Kirschner, *Polarized Electrons at Surfaces* (Springer, Berlin, 1985).
- <sup>36</sup>M. S. Altman, H. Pinkvos, J. Hurst, H. Poppa, G. Marx, and E. Bauer, *Proc. Mat. Res. Soc., Anaheim, CA* (1991).
- <sup>37</sup>E. Bauer and W. Teliëps, *Scanning Microscopy Supplement* 1, 99 (1987).
- <sup>38</sup>G. Rempfer, W. P. Skoczylas, and O. H. Griffith, *Ultramicroscopy* 36, 196 (1991).
- <sup>39</sup>W. P. Skoczylas, G. F. Rempfer, and O. H. Griffith, *Ultramicroscopy* 36, 252 (1991).
- <sup>40</sup>H. Leibl and B. Senftinger, *Ultramicroscopy* 36, 91 (1991).
- <sup>41</sup>W. Engel *et al.*, *Ultramicroscopy* 36, 148 (1991).
- <sup>42</sup>R. M. Tromp and M. C. Reuter, *Ultramicroscopy* 36, 99 (1991).
- <sup>43</sup>Y. Kondo *et al.*, *Ultramicroscopy* 36, 142 (1991).
- <sup>44</sup>C. E. Hall, *Introduction to Electron Microscopy* (McGraw-Hill, London, 1966).

## I. INTRO

The p  
trons is a  
both in a  
as well as  
surements  
depth pro  
tering len

In the  
the micro  
faces whic  
ular bean  
experime  
which exp  
and the a  
x-ray wav  
technique  
review se  
the invest  
Virtually  
have so t  
highly br  
scattering  
however,  
available,  
low evanc  
imental p  
tron scatt

Recei  
meter at  
Grenoble  
ambiguou

- <sup>45</sup>R. Castaing *et al.*, in *Focusing of Charge Particles*, edited by A. Septier (Academic, New York, 1967), p. 265.  
<sup>46</sup>H. Rose (private communication).  
<sup>47</sup>H. A. Enge, in *Focussing of Charge Particles*, edited by A. Septier (Academic, New York, 1967), p. 203.  
<sup>48</sup>V. Kolarik, M. Mankos, and L. Veneklasen, *Optik* **87**, 1 (1991).  
<sup>49</sup>A. Septier, *C. R. Acad. Sci. (France)* **235**, 652 (1952).  
<sup>50</sup>W. Engel, PhD. thesis, Berlin (1968).  
<sup>51</sup>M. Lenc (private communication).  
<sup>52</sup>G. F. Rempfer, *J. Appl. Phys.* **67**, 6027 (1990).  
<sup>53</sup>P. W. Hawkes, *Principles of Electron Optics* (Academic, London, 1989), p. 796.  
<sup>54</sup>J. J. Livingood, *Optics of Dipole Magnets* (Academic, New York, 1969), pp. 144-213.  
<sup>55</sup>S. Lanio, H. Rose, and D. Krah, *Optik* **73**, 56 (1986).  
<sup>56</sup>F. P. Ottensmeyer and J. W. Andrew, *J. Ultrastruct. Res.* **72**, 336 (1980).  
<sup>57</sup>E.g., Galileo Company, Sturbridge, MA 01566.  
<sup>58</sup>K.-H. Herrmann and D. Krah, in *Advances in Optical and Electron Microscopy*, edited by R. Barer and V. E. Cosslett (Academic, New York, 1984), Vol. 9.  
<sup>59</sup>E.g., Structure Probe Inc., West Chester, PA, catalogue p. 96.

- <sup>60</sup>D. Habliston, B. Baker, and O. H. Griffith, *Ultramicroscopy* **36**, 222 (1991).  
<sup>61</sup>K. H. Downing, *Science* **251**, 53 (1991).  
<sup>62</sup>A. V. Crewe, *J. Microscopy* **100**, 247 (1974).  
<sup>63</sup>L. Frank, *Vacuum* **42**, 147 (1991).  
<sup>64</sup>G. H. Jansen, in *Advances in Electronics and Electron Physics*, Supplement 21, edited by P. Hawkes (Academic, San Diego, 1990).  
<sup>65</sup>A. Brodie and D. W. Meisburger, *Microcircuit Eng.* 1991, Rome.  
<sup>66</sup>L. H. Veneklasen, *J. Vac. Sci. Technol. B* **3**, 185 (1985).  
<sup>67</sup>H. Lichte (private communication).  
<sup>68</sup>L. H. Veneklasen, *Optik* **44**, 447 (1975).  
<sup>69</sup>L. H. Veneklasen, *Proc. EMSA* 1991, San Jose, CA.  
<sup>70</sup>O. H. Griffith, P. A. Habliston, and G. B. Birrell, *Ultramicroscopy* **36**, 262 (1991).  
<sup>71</sup>G. B. Birrell, K. Hedberg, D. Habliston, and O. H. Griffith, *Ultramicroscopy* **36**, 235 (1991).  
<sup>72</sup>E. Bauer, M. Mundscha, W. Swiech, and W. Teliaps, *J. Vac. Sci. Technol. A* **9**, 1007 (1991).  
<sup>73</sup>E. Igras and T. Warminski, in *Electron Microscopy* (Rome 1968), edited by D. S. Bocciarelli (Tipographia Poliglotta Vaticana, Rome, 1968).  
<sup>74</sup>G. Rempfer, K. Kladakavukaren, and O. H. Griffith, *Ultramicroscopy* **5**, 437, 449 (1980).